EXPERIMENTAL STUDY OF SAND TRANSPORT AND DEPOSITION IN A HIGH-VELOCITY SURGE

by

PETER JOHN VROLIJK

B.Sci. Geology,
Massachusetts Institute of Technology
(1980)

Submitted in Partial Fulfillment

of the Requirements of the

Degree of

Includes
thesis.

MASTER OF SCIENCE IN GEOLOGY

at the

Massachusetts Institute of Technology

January 1981

Signature of Author _____
Department of Earth and Planetary Sciences
February 6, 1981

Certified by _____
J. B. Southard, Thesis Supervisor

Accepted by _____
Chairman, Department Committee

EXPERIMENTAL STUDY OF SAND TRANSPORT AND DEPOSITION IN A HIGH-VELOCITY SURGE

by

Peter John Vrolijk

Submitted to the Department of Earth and Planetary Sciences on February 6, 1981 in partial fulfillment of the requirements for the Degree of Master of Science in Geology

ABSTRACT

Experiments were made to determine the effects of sediment size, sediment concentration, and flow velocity on the depositional style of sand-sized particles in a high-velocity surge. A dimensional analysis of the experimental system was performed in an effort to relate the experimental results to deposits from turbidity currents and overwash surges.

A large part of each deposit was a result of deposition from suspension or mass emplacement. Fine and coarse sands are deposited primarily by mass emplacement, while medium sands result from deposition from suspension. These results suggested that grain size plays the dominant role in determining depositional style. Concentration has a lesser effect. For fine and medium sands, sediment volume concentrations of 20% and 40% were characterized by different styles of deposition.

Several mechanisms currently described in the literature used to explain features produced by high-velocity surges may have to be revised or discarded in light of the experimental results. Moreover, the development of interfacial instabilities and deformed beds as a result of turbulent eddies impinging on a liquefied bed may have important implications with respect to soft-sediment deformation and unusual types of grading, though these areas require extensive study.

Thesis Supervisor: Dr. John B. Southard

Title: Professor of Geology

TABLE OF CONTENTS

Table of Contents (Continued)

LIST OF FIGURES

ACKNOWLEDGEMENTS

This section of a thesis is perhaps the most difficult to put on paper. The apology that time and space do not permit an adequate thanks of all people involved in the preparation of this document takes on a very real meaning. The best reward I can offer these people is the personal satisfaction that they have aided me in what is hopefully a contribution to the field of sedimentology.

I would like to offer very special thanks to my advisor, John Southard, who offered assistance and encouragement during the particularly low points in construction of the apparatus, stimulation and excitement when the project seemed to loom too large, reassurance and calm words of advice during the sometimes chaotic production of this manuscript. I also have to thank John for interesting me in geology at the undergraduate level; John is perhaps the single greatest asset of the department at this level.

Don Argus and Peter Southard deserve special thanks for assisting me in the experiments. When one considers that, on the average, 800 lbs. of sand had to be lifted over ten feet in the air for each experiment, this acknowledgement is small thanks.

The distinguished members of the Center for Experimental Sedimentology were invaluable in lending assistance and advice. Keven Bohacs, Bill Corea, Roger Kuhnle, Dave McTigue, and Chris Paola assisted this research in one way or another by thoughtful discussions. My good friend Doug Walker helped me perhaps more than anyone in many different aspects of the project, and our faces will not soon be forgotten at the Vouros Bakery.

Other members of the tenth floor contingent that I would like to recognize include the "Clones", many of whom sat through several movies with me, and especially John Bartley and Kip Hodges; Ana Silfer and Marilyn Copley provided support in the true meaning of support staff. Others who aided in the preservation of my sanity are B.J. Pegram, Julie Morris, and Tansy Mattingly. I also wish to thank Cathy Lydon for typing the manuscript.

Bill Chesterson drafted drawings of the apparatus in the manuscript and designed and built many of the key parts of the surge tank, and he was often assisted by Ed Insel. Bill helped me night, weekends, whenever he was needed.

To go back to the beginning, I must thank Steve Leatherman of the National Park Service for bringing the problem of unusual grading patterns in overwash deposits to our attention. His studies launched this

project.

Three people who know very little about geology contributed very much toward the completion of my studies. My parents, Jacobus and Janet Vrolijk, supported me through more than four years of school. Karen Bauer, my future wife, comforted me and cared for me through the last difficult period of this research.

Funding for the construction of the surge tank came from the Undergraduate Research Opportunities Program. The Student Research Fund provided valuable funds that allowed the experiments to be made. The College Work-Study Program provided support for my last semester of school. The departmental thesis fund helped me considerably in preparing this manuscript, and I am especially indebted for the award that permitted copies of my movies to be preserved in the archival collection.

INTRODUCTION

Deposition of sands from high-velocity, high-concentration surges has received attention in regards to both subaqueous and subaerial flows, the notable examples including turbidity currents and storm surges in a barrier-beach environment. Much work has been done on the hydraulics of the flow, the competence and capacity of flows, and the sedimentary record of such flows (see for a review of the literature: Middleton, 1970: Walker, 1970; and Leatherman, 1977). However, with the notable exception of Middleton (1967), no work has been done in a quantitative or even qualitative manner to describe the physical processes of the transport and deposition of sand-sized particles. According to Middleton (1967),

> There have been very few experimental studies of turbidity currents bearing coarse sand and, in those experiments, the nature of the apparatus and sediment that were used made it very difficult to observe the actual mechanisms of deposition.

An experimental study of the processes involved in deposition of sand from a high-velocity surge would, therefore, go far in bridging the gap between the understanding of the hydraulics of high-velocity surges and the sedimentary record left by such flows. How are the massive sands found in turbidites produced? Can different degrees of grading be related to different surge conditions? Many

more questions along this line can be posed, but ultimately the question to be asked is: how is the bed deposited as a function of varying flow conditions? By changing the grain size, concentration,and velocity, is it possible to determine if the bed is deposited (1) in a tractional mode, whereby the grains come to rest at some time after being rolled along the bed, (2) by settling of individual grains from the fluid suspension and subsequent burial in the bed with no tractional movement, (3) by mass-emplacement, whereby the grains come to rest to form a highly concentrated, fluidized bed in which there is little motion relative to neighboring grains, or (4) by some combination of these mechanisms?

This study examines the modes of deposition of three different sand sizes,0.25,0.44,0.54 mm, as a function of velocity and sediment concentration. A series of 16 mm slow motion movies were made to record and document depositional processes in each run and are described in this report. Sediment samples were also taken after each run to examine how the size distribution of the sediment changes with varying flow conditions.

Discusson of Literature

Kuenen (1950) pioneered the experimental study of high-concentration surges,but his primary interest

was in the erosive processes and capabilities of such flows, and not in the depositional characteristics. In later experiments (Kuenen, 1951) his attention shifted more toward the transporting power of turbidity currents and paid only token attention to depositional features. Not until the revolutionary paper by Kuenen and Migliorini (1950), which was inspired by Kuenen's paper at the Eighteenth International Geological Congress in 1948 (Kuenen, 1950) did the connection between high-concentration surges and the deposition of sand arise. Graded bedding, recognized as an important part of the sedimentary record, was suggested to be a result of deposition from turbidity currents. Kuenen also reported the occurrence of experimentally produced graded beds in Kuenen and Migliorini (1950), tightening the link between graded deposits and turbidity currents. Kuenen and Migliorini also made the first step toward describing the mechanism of deposition (p. 122): "Because the flow drops its load from suspension and hardly moves it along the bottom afterward, no cross-bedding is developed."

This idea was modified by Kuenen (1953) when it became obvious that transport of some part of the deposited bed was occurring since bed forms were recognized in turbidites. The explanation given is that for one part of the depositional episode, sediment is being deposited directly from the flow, and for the other part, sediment is moved by

traction on the bed. The boundary between the depositional regimes occurs when the "high" density flow becomes diluted to become a "low" density flow. This somewhat vague notion will be seen to become very important in subsequent studies.

In the mid-1960's, Middleton conducted a series of experiments that sought to explore the hydraulics of density flows as they relate to turbidity currents, and to describe the transport and deposition of sediment in a turbidity current. Middleton (1967) described the transport and deposition of plastic beads ($\rho = 1.52$ g/cm^3, $D = 0.18$ mm) suspended in water as a function of velocity and concentration. After several initial experiments it was determined that flows above 30% concentration behaved radically differently than those below 30% concentration. The experiments were, therefore, performed with flows of around 23% (low) and 44% (high) volume concentration.

Sampling of the bed demonstrated that graded beds were being produced. In beds formed from low-concentration suspensions, "distribution grading" developed, in which all percentiles showed vertical grading, but the coarser half showed downcurrent grading also. High-concentration flows formed beds displaying "coarse-tail grading," where no downcurrent size variation was noted, and only the coarsest few percentiles (1-5%) showed vertical grading; however, the topmost part of the bed did show distribution grading.

Some aspects of the grading were similar in both cases. For example, sorting improved both vertically and horizontally in a particular bed, and the skewness reached a maximum at the center of the bed but became negative at the top. The basal section also tended to have a finer median grain size than the next successive bed and was more poorly sorted, especially in the high-concentration flows. Several explanations were given for this phenomenon, but the one favored by Middleton suggests that mixing and turbulence just behind the head of the flow may prevent size segregation, resulting in a basal sample being an "undifferentiated sample."

The mechanism of deposition in both the high and low concentration cases can be broken down into four discrete phases,with only the final phase common to both cases. In the low-concentration case, sediment began to be deposited very shortly after the passage of the head. The first grains were deposited directly from suspension with little or no traction along the bed, contributing to only a small part of the thickness of the entire bed. A period of slow deposition of sediment from suspension followed,with traction on the bed a much more important feature. Sediment was deposited in a grain-by-grain or layer-by-layer manner from dense clouds of suspension. Most of the sediment was deposited in the third phase, which is characterized by

rapid deposition due to depletion of the supply of suspension resulting in a decrease in the velocity of the current. This depletion is related to dissipation of the hydraulic head which drives the flow. The final phase is characterized by very slow deposition of the finest sediment from the "tail" of the current.

Deposition in the high-concentration case was markedly different. Grains were again deposited shortly after the passage of the head, but these particles had a greater chance of being retransported, not by rolling along the bed, but by shearing of the bed; it was also difficult to define the top of the bed at this point. The second phase of bed development is recognized by the definition of the top of the bed. The bed appears in an expanded, "quick" form, about 30% thicker than the final thickness. A disturbance in the interface between the fluidized bed and the flow above produces, in Middleton's terminology, Helmholtz waves (Prandtl, 1952, p. 50-53). As these Helmholtz waves pass downstream, a circular shearing develops in the upper two-thirds of the bed. The velocity then begins to drop, the waves disappear resulting in a plane surface, and the bed consolidates.

Middleton concluded that the difference between high-concentration flows and low-concentration flows appeared to be a result of the limitation of size segregation in the

high-concentration flows. The concept of "dispersive pressure" (Bagnold, 1956) was suggested as a mechanism for this limitation; the upward normal force (or dispersive pressure) produced is maintained by the high shear stress acting on the unconsolidated bed and works to prevent or delay consolidation of the bed as it was being formed by mass settling. The shearing at the top of the bed was a result not of the turbidity-current flow, which had already ceased, but of the overlying fluid that became "entrained" as the turbidity current passed and continued to flow as a result of inertia. The velocity of the "entrained" flow can approach the velocity of the turbidity current.

The manner in which the bed consolidated once the velocity of the entrained fluid decreased, causing a decrease in shear stress, is also interesting. A highly concentrated sediment-water mixture behaves as a pseudoplastic, and when the shear stress is high and the viscosity relatively low (sediment:water≈1:1), the mixture can be treated as a Newtonian fluid. Once the shear stress decreases as a result of a decrease in the velocity, the viscosity will increase and a yield strength may be achieved. Middleton claimed that this effect will be accentuated and accelerated when a coarse suspension in a gravitational field is considered, and also when dispersive pressure is taken into

account. He reasoned that as the shear stress decreases, so too does the dispersive pressure (Bagnold, 1956), leading to settling of the sediment; this increases the concentration and subsequently the yield strength. As a result a sediment-water mixture will "freeze" even more rapidly than a pseudoplastic.

Sedimentary Deposits of Sand From a High-Velocity Surge

The most voluminous deposits from high-velocity surges are most certainly found in turbidites. Sand-sized particles are most commonly found in the graded interval, or "a" interval of Bouma (1962). Bouma (1962, p. 49) described this interval:

> The bottom part of the layer consists of sand, showing a more or less distinct graded bedding. This grading may be indistinct or even absent if the material is well sorted. The texture of this interval is sandy and sometimes gravel and pebbles may be found. No other characteristic structures are known in this interval.

However, a different type of deposit, an overwash deposit, produced by storm surges in a barrier-beach environment, while not nearly as important in the rock record, may be at least qualitatively similar in hydrodynamic and depositional characteristics. It may be studied and referred to in examining the depositional properties of a high velocity surge.

Overwash hydraulics and associated sediment transport have been discussed by Leatherman (1977). An overwash event

has been described by Leatherman (1977):

> Areas along the barrier dune line are weakened and/or lowered by blowouts and vehicular passage serve as avenues for penetration of the swash. Overwash is defined as the transport of sea water and associated sediment from the beach face to the backdune area.
>
> As the overwash surges proceed between the dune gaps, sediment is eroded from the throat and transported landward for deposition on the fan.

Overwash deposits form a series of graded beds up to 2-3 m thick with individual beds on the order of 1-2 cm thick (Leatherman, personal communication). Overwash deposits may, however, form normally graded or inversely graded beds.

THEORETICAL CONSIDERATIONS

The theory of dimensional analysis was introduced by Buckingham (1914) as a theorem in applied mathematics. From its inception the theorem's applicability has spread greatly. Engineers immediately grasped the significance of the concept; modelling of physical systems from one scale to another scale has been used in all areas of engineering.

The usefulness of dimensional analysis and scale modelling in the field of sedimentology has only just recently become recognized. Dimensional analysis is particularly useful because it reduces the number of physically pertinent variables needed to describe a physical system. Scale modelling, on the other hand, allows one to take the dimensionless analysis, evaluate these variables for a particular system, and then by keeping the dimensionless variables constant, model that system from one scale to another by altering the dimensional variables. A test of scale modelling for ripples is given by Southard, et al (1980).

Dimensional Analysis

Six independent variables govern the flow and sediment deposition in the experimental surge tank: C, the initial sediment volume concentration; H, the hydraulic head height; ρ, the density of the fluid; μ, the fluid viscosity;

D, the mean grain size of the sediment; and g, the acceleration to gravity. The implicit assumptions in generating this list include the characterization of the flow as two-dimensional, thereby disregarding the width of the channel, and the idea that the sediment shape and sorting are not important; it is also given that the slope of the channel does not change.

The dimensions of the six independent variables are mass, length, and time, so the Buckingham Pi theorem indicates that three dimensionless variables must be derived, which can be:

$$C, \frac{\rho^2 g D^3}{\mu^2}, \frac{\rho^2 g H^3}{\mu^2} .$$

C, the initial concentration, is dimensionless in the first place. $\rho^2 g D^3/\mu^2$, the materials number, can be regarded as a dimensionless quantity describing the physical characteristics of the flow. $\rho^2 g H^3/\mu^2$ can be viewed as a dimensionless head height.

The number of variables necessary to accurately describe an experimental surge has been reduced from six to three, a much more manageable number. Now considering the experiments were run in an earth-bound system, gravity can be assumed to be constant and equal to 980 cm/sec^2. The fluid density can also be assumed to be constant because the density of water varies only slightly with different

conditions of temperature, salinity, and so forth. The fluid viscosity was varied only slightly as a function of temperature which changed from run to run; it seems reasonable to hold the viscosity relatively constant because the viscosity of water varies mostly with temperature, and then well within an order of magnitude.

The variables that seem most realistic to vary are the initial sediment volume concentration, the mean sediment grain size, and the hydraulic head height. The range of variability for the experiments is given in Figure 1, both in terms of dimensional and dimensionless variables.

Comparison of Natural and Experimental Flows

Comparison of turbidity currents and overwash surges with the experimental surges is essential in determining if the results derived from the experimental study are applicable to the natural cases. At first glance the flows are only grossly similar in detail. For example, the effect of the slope is probably greater in a turbidity current than an overwash surge, while in an experimental surge it does not exist at all. The processes involved in the generation of a turbidity current are extremely complex, the details of which probably cannot be estimated on a first-order basis; the same is largely true for an overwash surge. These effects must, therefore, be examined on a scale where all the relevant parameters are definable and where the

FIGURE 1: Dimensional and Dimensionless Variables from Experiments

FIGURE 1

	C	D(mm)	T(°C)	μ ($\times 10^{-3}$ g/cm-sec)	H(cm)	$\frac{\rho^2 g D^3}{\mu^2}$	$\frac{\rho^2 g H^3}{\mu^2}$
A-1	20%	0.44	26°	8.705	244	9.55	1.88×10^{14}
A-2	20%	0.44	25°	8.904	168	9.38	5.86×10^{13}
A-3	40%	0.44	23°-24°(?)	~9.2	244	9.07	1.68×10^{14}
A-4	40%	0.44	28°	8.327	168	10.03	6.70×10^{13}
B-1	40%	0.54	26°	8.705	168	17.73	6.13×10^{13}
B-3	20%	0.54	25°	8.904	244	17.33	1.80×10^{14}
B-4	20%	0.54	30°	7.975	168	19.35	7.31×10^{13}
B-5	40%	0.54	34°	7.340	244	21.02	2.64×10^{14}
C-1	20%	0.25	25°	8.904	244	1.72	1.80×10^{14}
C-2	20%	0.25	24°	9.111	168	1.68	5.60×10^{13}
C-3	50%	0.25	32°	7.647	244	2.00	2.43×10^{14}
C-4	40%	0.25	30°	8.975	168	1.92	7.31×10^{31}

large-scale processes that cannot be defined have little or no effect. A shortcoming of these experiments is that some of the mechanisms that are being overlooked may have a profound effect on the processes studied, but there is no quantitative way to evaluate these effects. Intuition and experience must be the guide in this case. The writer's feeling is that this approach is valid.

Since the mechanisms governing the evolution of the different flows and some of the processes involved in the flows are not comparable, it seems reasonable to choose a point and a scale that are largely unaffected by these other processes. For this study a point will be selected where sand is actively being deposited, and the temporal variations in depositional style will be studied in an Eulerian reference frame. The relevant system variables at this point are U, a measure of velocity; d, the flow depth; C, the volume concentration of the sediment in the flow; ρ, the density of the fluid; μ, the viscosity of the fluid; g, the acceleration due to gravity; and D, the mean grain size (Figure 2).

The next step is to derive a series of dimensionless variables which can be computed in each of the three cases and compared to each other. The Buckingham Pi theorem indicates that since seven variables and three dimensions are represented, four dimensionless variables

FIGURE 2: System Variables in General High-Velocity Surge

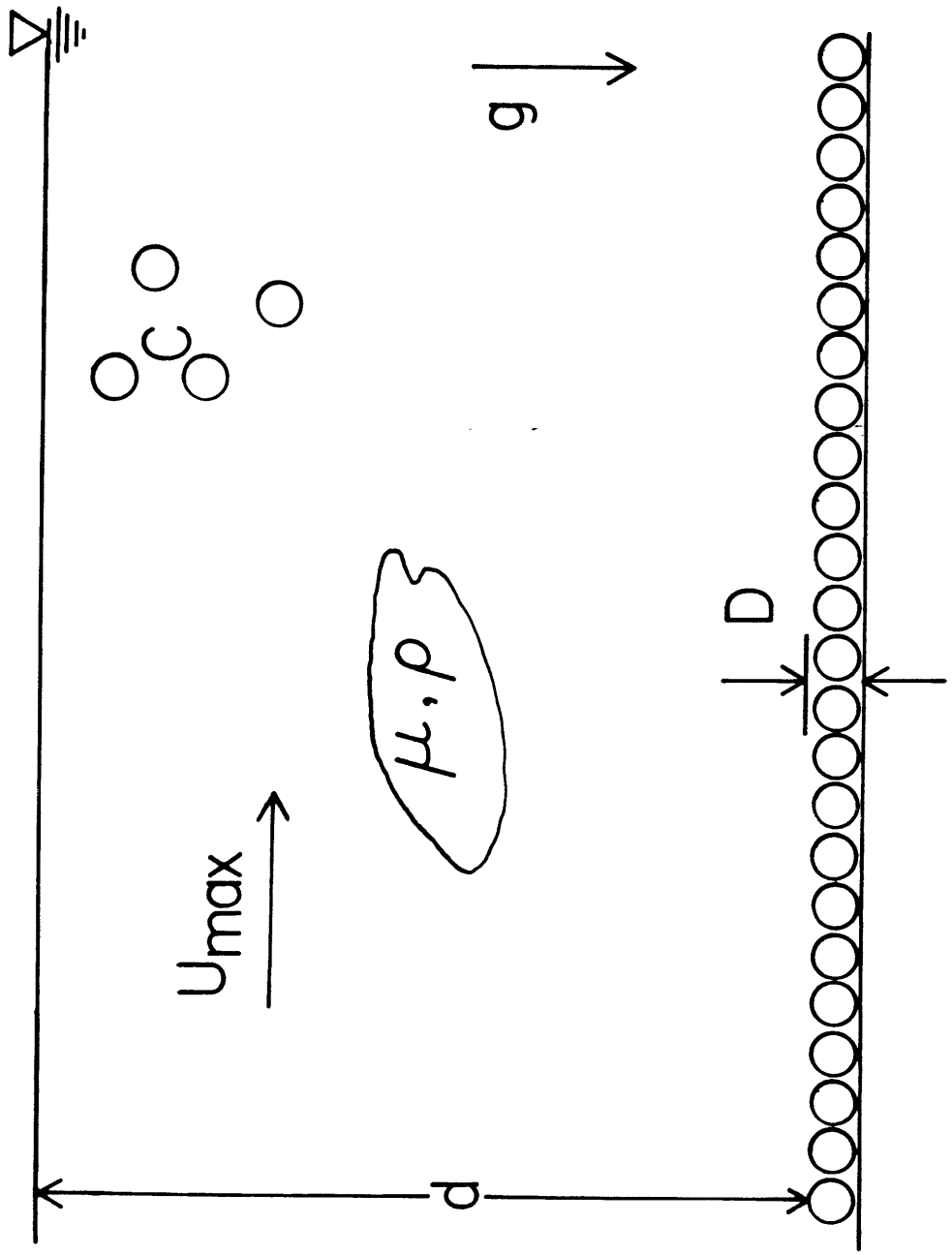

Figure 2

must be derived. These are

$$C, \frac{\rho U d}{\mu}, \frac{\rho^2 g D^3}{\mu}, \frac{d}{D}$$

which will be referred to as the concentration, the Reynolds number, the materials number, and the length ratio, respectively.

Computation of these numbers will require a degree of intuition and some order-of-magnitude arguments. I have explained earlier that ρ and μ vary only slightly in most natural systems, so values of 1 g/cm^3 and 10^{-2} poise, respectively, will be applied in all calculations. Measures of the other values on the scale I have chosen are next to impossible; for example, the depth of the part of the flow from which sand is being deposited cannot realistically be evaluated. For computational purposes maximum values of flow conditions will be chosen at a point near the point of study. While this approach detaches the evaluation of the dimensionless variables from the point of study, it provides a ground on which arguments can be based. Qualitatively, this approach seems reasonable.

In the case of turbidity currents, estimates of the flow depth and velocity must be made. Kuenen and Migliorini (1950) report that experimental turbidity currents were produced with velocities ranging from 67-83 cm/sec while

Menard (1964) has estimated the velocity of the Grand Banks turbidity currents of 1929 to range from 10-20 m/sec. Komar (1977) has argued that velocities of 7 m/sec are competent to transport gravels and cobbles. It would seem likely, then, that sand is deposited by currents velocities of approximately 1-5 m/sec. The depth (d) of a turbidity current flow is also quite difficult to estimate. Komar (1977) reasons that flows are probably less than 100-200 m deep, but may be as deep as 300 m, though these values seem a bit high. Menard (1964, p. 204), on the other hand, has estimated flows on abyssal plains to be tens of meters deep. A flow depth of about 10-50 m seems reasonable in this light. The flow Reynolds number is, therefore, $Re = 2.5 \times 10^8$. The materials number, assuming a medium sand grain size (D = 0.4 mm), is equal to 6.27×10^2. The length ratio is 1.25×10^5. Geologic evidence suggests that the concentration of turbidity currents might range from a value necessary to produce the current, presumably fairly low, up to about 65%, the maximum for flow of the mixture. Intuitively it seems reasonable to restrict the majority of flows to 10%-50%.

An overwash surge is more easily measured, and quantities can be more easily estimated and recorded. Leatherman (1977) has measured surges ranging from 1-3 m/sec with

the average maximum velocity being 1.95 m/sec. The flow depth ranges from a "few inches to four feet, the average being one to two feet" (0.30 m - 0.60 m). The density and viscosity can be estimated as in the turbidity current case to be 1 g/cm^3 and 10^{-2} poise, respectively. A medium sand (D = 0.4 mm) will again be assumed in computing the three dimensionless variables: Re = 1.19×10^7, $\rho^2 gD^3/\mu^2$ = 6.27×10^2, $d/D = 1.53 \times 10^4$. Again the concentration can vary over a wide range of conditions (10%-50%).

A list of the measured fluid properties from the experiments is presented in Figure 3. The viscosity was computed as a function of water temperature only; an estimate of the temperature is given in Run A-3 because the thermometer was broken just before the run, and a replacement was not available. The flow depth and velocity were calculated from films by a technique which will be described in a later section. No readings are given for Runs A-1, A-2, and A-4 because Camera B was malfunctioning at the time, and the error was not realized until after the films were developed. The velocity in Run B-4 was not recorded because no Styrofoam balls passed the field of view of the camera; in the other cases the number of balls from which the velocity was computed is given in parentheses.

Comparing the computed values of the dimensionless variables reveals that these systems cannot be modelled in

FIGURE 3: Measured Dimensional Parameters and Derived Dimensionless Variables from Experiments.

FIGURE 3

	U_{max} (cm/sec)	d (cm)	D (mm)	μ ($\times 10^{-3}$ g/cm-sec)	C	$Re=\frac{\rho U_{max} d}{\mu}$	$\frac{\rho^2 g D^3}{\mu^2}$	$\frac{d}{D}$
A-1	--	--	0.44	8.705	20%	--	9.59	--
A-2	--	--	0.44	8.904	20%	--	9.38	--
A-3	320(4)	17	0.44	~9.2	40%	5.91×10^5	9.07	3.86×10^2
A-4	--		0.44	8.327	40%	--	10.03	--
B-1	284(1)	11	0.54	8.705	40%	3.59×10^5	17.73	2.04×10^2
B-3	366(2)	20	0.54	8.904	20%	8.22×10^5	17.33	3.70×10^2
B-4	--	16	0.54	7.975	20%	--	19.35	2.96×10^2
B-5	366(4)	18	0.54	7.340	40%	8.98×10^5	21.02	3.33×10^2
C-1	366(4)	18	0.25	8.904	20%	7.40×10^5	1.72	7.20×10^2
C-2	284(3)	15	0.25	9.111	20%	4.68×10^5	1.68	6.00×10^2
C-3	320(2)	19	0.25	7.647	50%	7.95×10^5	2.00	7.60×10^2
C-4	259(2)	9	0.25	7.875	40%	2.89×10^5	1.92	3.6×10^2

the strict sense of the term because the Reynolds number and length ratio both differ by up to three orders of magnitude between the turbidity current flow and the experimental surges. However, I believe the systems are qualitatively similar and can be related on a first-order basis because in all cases the Reynolds number indicates fully turbulent flow; the presence of strong turbulence is probably one of the greatest factors in the characterization of these flows. The length ratio is similarly affected by the depth of flow, but in the turbidite case this value is perhaps most poorly constrained and may be less. In any case, a difference exists, and this difference will be most apparent in the size of turbulent structures allowed to develop in the flow. I believe this factor may affect the depositional processes in detail, but not necessarily in general.

I, therefore, propose that the processes governing the deposition of sand from different high-velocity surges can be related in a grossly similar fashion. The exact details and mechanisms might not be the same, but the overall processes are similar in all three cases. Most importantly, in all cases the conditions are reasonably and qualitatively similar near the bottom where the depositional process is probably most strongly affected. The local near-bottom shear stress, the turbulence, flow velocities, and sediment concentrations are in all cases qualitatively similar.

PHYSICAL DESCRIPTION OF THE SYSTEM

Surge Tank

The experiments were made in an open, rectangular, horizontal channel 9.75m long with a 0.6 m x 0.6m cross-section (Figure 4). The channel empties into a small (1.2m x 1.6 m) box which serves as a flow expander to trap the coarse particles still remaining in the surge and to turn the surge 90° into a large (2.4 m x 4.9 m) collection box.

The hydraulic head of the surge is produced in the head tank, a vertical tank 2.4m high with a 0.6 m x 0.6 m gate at the bottom of the tank; opening and closing of the gate is facilitated by a hand winch mounted on the top of the head tank. Also on the top of the head tank is a shallow, square box, 1.8 m long x 0.6 m high. Half of this volume is used as a sediment hopper box in which the sediment for a particular run is stored. The other half is open and provides space for the operator to open and close the gate, control the input of water, measure the water temperature, and release the sediment into the water.

The channel was constructed from 1/4" and 3/8" particle board with 3" x 8" supports every 0.4 m along the channel. The channel rests on 4" x 4" pine supports laid lengthwise along the channel. The seams were sealed by strips of fiberglass matting with a polyester resin coating; the

FIGURE 4: Diagram of Surge Tank

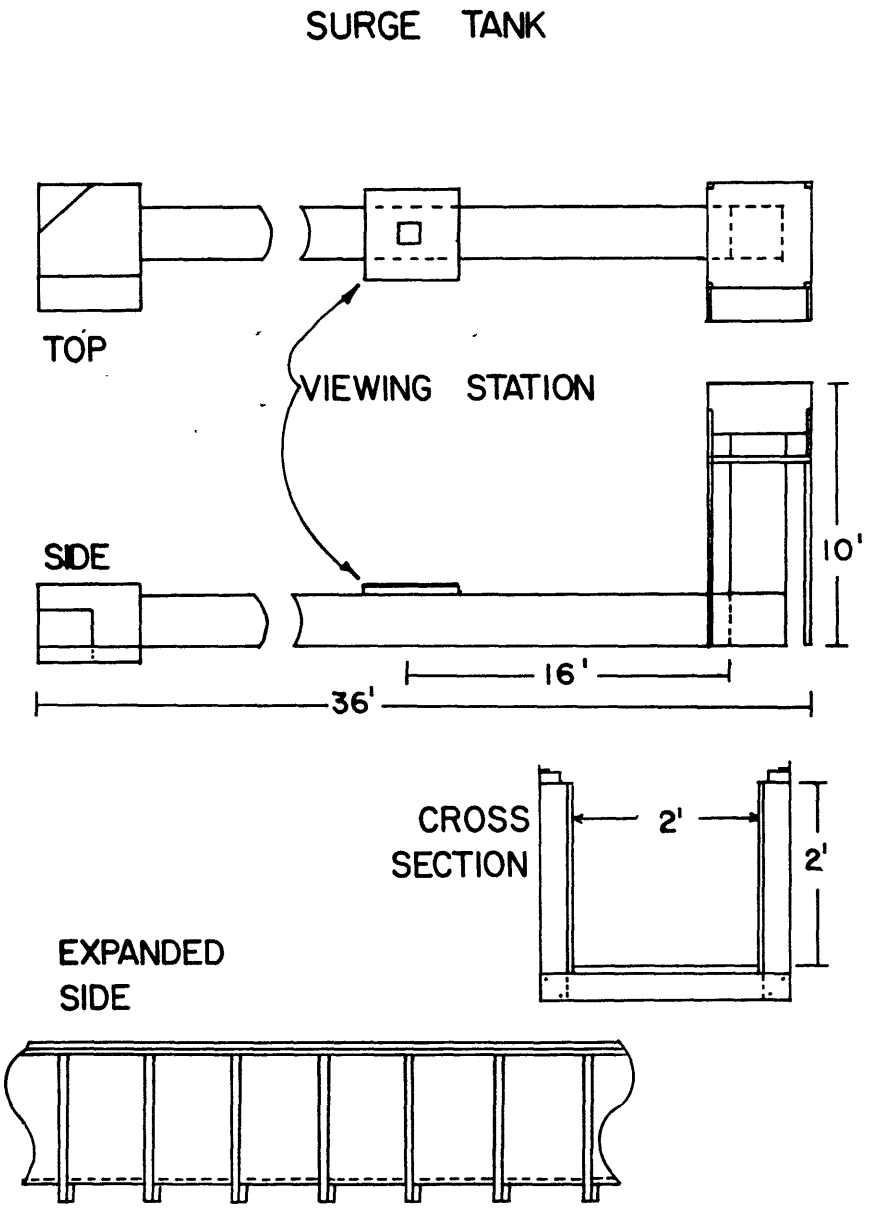
SURGE TANK
TOP
VIEWING STATION
SIDE
10'
16'
36'
CROSS SECTION
2'
2'
EXPANDED SIDE

Figure 4

particle board was waterproofed with the same resin. The flow expander box at the end of the channel was constructed from similar materials.

The collection box consists of a wooden frame constructed from 3" x 8" and 1/8" plywood, with two sheets of 3 mil polyethylene plastic draped within the frame.

The head tank and the shallow box on top were constructed from 1/4" AD plywood with 2" x 4" supports (serving as horizontal strap supports) placed every 0.4 m. The seams were similarly sealed with fiberglass matting and resin. The floor of the head tank was reinforced with two sheets of 1/2" plywood glued and screwed together. The box on the top of the head tank was also reinforced, first by four 2.6 m long 4" x 4" pine supports placed at each corner of the box, and second by a steel chain wrapped underneath the box and fastened to the ceiling I-beam supports.

The sediment hopper box was built inside the larger box. The flocr was tilted at 30° toward the opening to ensure that all the sediment in a particular experiment was used. The gate was constructed from 3/4" plywood and is hinged by four 2" x 2" door hinges to the top of the head tank. The release was fashioned from two steel pins which, when rotated into the proper position to align them with slots in the gate, allowed the gate to open freely and

empty the sand in several seconds. Sand is loaded into the hopper by means of a bucket that is raised and lowered by a rope and pulley mounted to the ceiling.

The gate that releases the flow was made from 3/4" plywood coated with polyester resin and reinforced with steel supports. The inner side had a sheet of 1/8" thick Neoprene rubber glued to the plywood with a rubber cement to enhance the seal. The gate is hinged by three steel barn hinges to the gate's frame; the hinges were reinforced by pieces of steel angle welded to the hinges. A steel I-beam along the bottom of the gate serves as reinforcement and an anchor for the eye bolt to which a 1/8" steel cable is attached. This cable runs horizontally to a galvanized marine steel pulley fastened to the back wall of the tank, and then vertically to the hand winch.

The most time-consuming and frustrating phase of construction of the apparatus came in devising an adequate seal for the gate. Many different ideas were attempted, but the method that ultimately worked consisted of a stapling a gasket of 1/4" open-cell foam rubber on the gate frame after a coat of transparent silicone caulking had been spread on the frame. The seal between the Neoprene rubber on the gate and the foam rubber on the frame is essentially leak-proof.

Flow Viewer

The movies of sediment transport and deposition and the velocity and depth profiles were taken at a point 4.85 m downstream from the head tank. The movies of transport and deposition were made through a "flow viewer", simply a streamlined periscope which allowed movies to be made of the surge with no disturbance to the flow in the viewing section and which also allowed observations to be made of the mechanisms only slightly affected by the boundary layer at the wall. The original idea was to build a streamlined body with a knife-edge so that a turbulent boundary layer would begin to grow continuously at that point. A carefully machined wedge with a small angle was decided upon as an appropriate knife-edge. The side from which the movie would be made should be flat and parallel to the flow direction while the back side would taper away slowly from the viewing side for about 10cm, and then bulge out so that at the widest point the two sides would be 7.75 cm apart. The back wall would then taper back to join the viewing wall. The ensuing design resembles two airfoils superposed with one facing in the opposite direction of the other, and the bulbous parts overlapping (Figure 5).

The distance from the knife-edge to the viewing point had to be as small as possible to keep the boundary layer

FIGURE 5: Diagram of Flow Viewer

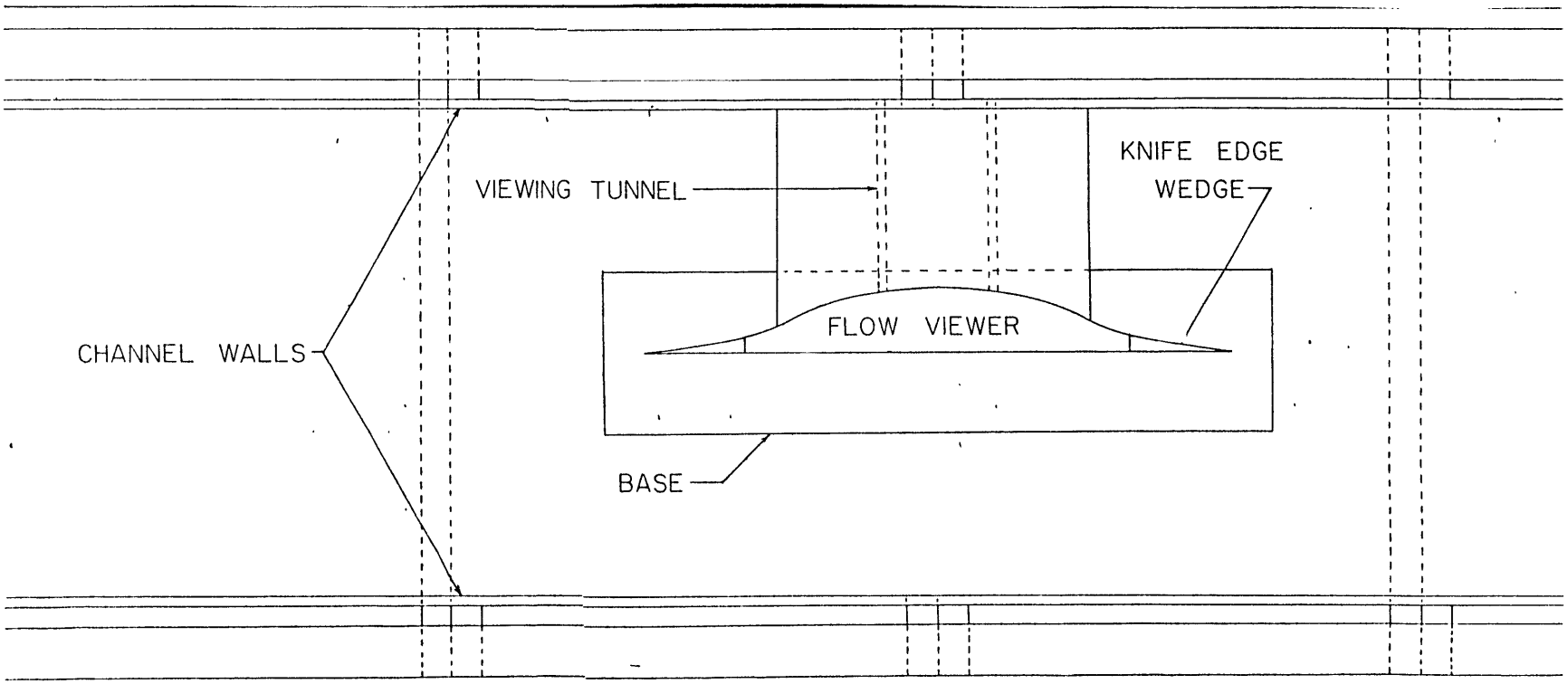

TOP VIEW OF FLOW VIEWER (PLATFORM OMITTED)

Figure 5a

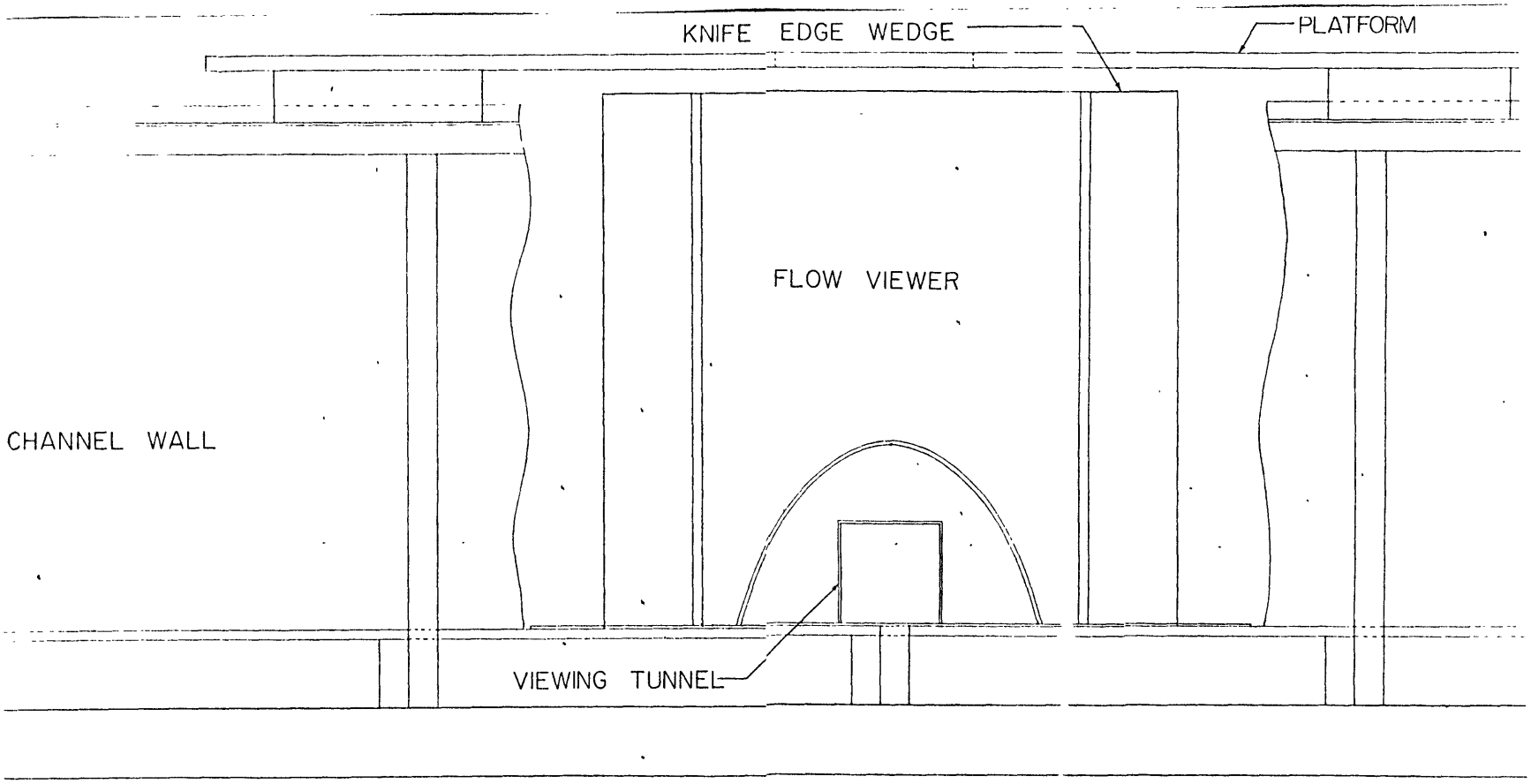

SIDE VIEW OF FLOW VIEWER IN CUTAWAY OF CHANNEL

Figure 5b

thickness (δ) small. This was calculated from the boundary layer thickness equation (Fox and McDonald, 1978):

$$\frac{\delta}{x} = 0.370 \left(\frac{\nu}{U_o x}\right)^{1/5}$$

where x is distance along the wall, ν is kinematic viscosity, and U_o is mean flow velocity. For example, for values of $x = 0.25$ m, $\nu = 8.904 \times 10^{-7}$ m^2/sec, and $U_o = 2$m/sec; $\delta = 0.66$ cm. Using the worst case from the experiments, $\delta = 0.56$ cm.

The flow viewer was built from 1/8" Plexiglas walls glued to machined aluminum knife-edge wedges with an angle of 10°. Two 1/8" grooves were machined into the aluminum so that the Plexiglas could be joined to the wedge. The back wall was heat-formed to obtain the desired shape. A mold was first constructed of masonite and particle board. The Plexiglas was then heated to 190°C in a commercial oven for fifteen minutes, and finally placed on the mold and allowed to drape over the form until cool. The results were remarkably pleasing. All parts were glued with 5-minute epoxy and allowed to dry before the viewer was mounted on a Plexiglas base.

After the viewer was placed in the surge tank and tested to assure the angle of attack was correct, a plywood platform

with a hole in the center was mounted on top of the viewer and attached to the wall of the surge tank for two reasons: 1) to allow a worker to maneuver on top of the viewer with ease, and 2) to ensure that the viewer was stable and would not undergo any vibrations as the surge passed. Two adjustable mirrors were then emplaced such that light from a Mole-Richardson Junior Solarspot spotlight with a 2000 W bulb mounted above the flow viewer could be reflected by a single mirror to illuminate the viewing section. This image would be reflected by the second mirror and recorded by a Bolex H16 Reflex movie camera (Camera A), also mounted above the flow viewer. This arrangement was tested and rearranged and retested, but it become apparent that due to the space constraints it was not possible to illuminate the test section properly.

The flow viewer was thus modified so that it would be possible to have adequate illumination and preserve the advantages of a streamlined viewer. A tunnel was therefore built connecting the back wall of the viewer and the wall of the channel. The camera then looked straight through the tunnel and at the test section while light was shone through the viewer from above. Streamlining of the tunnel helped to reduce the adverse flow effects, though none of these effects appear to be evident during most of the

depositional process. This arrangement seemed to work the best and was used for the experiments.

Velocity and Flow Depth Profiles

The last bit of construction involved a system to measure flow depth and velocity. A crude arrangement was devised that would produce qualitatively accurate measurements. First the wall adjacent to the viewing station was painted white, then a vertical scale was painted in black on the wall with 1 cm thick lines marked 6 cm apart (from base of line to base of line). Two 1 cm thick, black vertical lines spaced 20 cm apart served as a horizontal scale. At a point 3.0 m from the gate (and upstream of the scale), an inclined 3" ID pipe was mounted with a hinged gate on the lower side and four 3" Styrofoam balls were loaded into the pipe. Therefore, when the flow passed, the gate could be opened, the balls would roll out and float on the surface, and the free-stream velocity could be measured by noting the time required for each ball to pass the 20 cm between the vertical markings. Accuracy would be enhanced by filming the flow at 64 frames/sec and analyzing the film produced, so a Paillard-Bolex H8 movie camera (Camera B) with a Kern-Paillard 75 mm telephoto lens, was mounted 2.90 m from the wall and with the line of sight forming approximately a 45° angle with the horizontal. A telephoto lens was employed to reduce any

parallax effect (Southard, 1966).

Physical Drawbacks of Apparatus

Several flaws in the design of the apparatus became apparent after experiments began. A small wave was found to travel upstream during the waning stages of flow as a result of the flow being reflected in the turning box at the end of the channel. Observations indicate that this wave reaches the viewing station after almost all of the sediment has been deposited, so it is of small importance.

A much more important wave is generated at the flow viewer as the flow directed to the back side of the viewer decreased in depth and velocity to a point where water can no longer travel over the streamlined tunnel between the viewer and the wall of the channel. The water backed up on this side of the viewer, causing an increase in flow depth at the viewing window and an accelerating flow past the window due to the channel expansion past the window. Fortunately, though, this effect appeared to be limited in most cases to the waning stages of flow when most of the sediment has been deposited.

The method for determining flow velocity also did not perform as well as expected. It was hoped that in each run all four balls would be photographed so that the temporal variation in velocity of the surge could be examined. Un-

fortunately, the balls commonly drifted out of sight. The failure of Camera B in the first set of experiments also limited the value of such an exercise.

The ability to produce a uniform initial suspension in which no segregation of grain sizes occur was limited by the amount of sediment in any particular experiment. A 3/4 horsepower centrifugal pump was initially installed in the head tank to produce circulation cells with a net upward mass transport, but it became evident that much sediment was still settling out of suspension. The sediment hopper box that was used in all of the experiments was then built and the pump used as a supplement in preventing the mass settling of grains. Although the exact mechanism by which the sediment was dispersed through the water column is unclear, it can be assumed that the sand fell as a plug with the outer edges being continuously sheared off. A reasonable amount of sediment was probably deposited on the floor of the head tank, but it seems likely that if the gate to the tank was opened very shortly after the sediment was released, the deposited sediment could easily be resuspended. From observations at the viewing station it appeared that this method, while far from ideal, ultimately produced the desired sediment suspension in a fully turbulent flow. Description of the experiments in a subsequent section will reinforce this premise.

Experimental Procedure

It might be appropriate at this point to discuss generally how a run is made. The first thing done is to make sure the seal around the gate is tightly closed. Four 5/8" (1.6 cm) garden hoses feed the water into the head tank until the desired water depth is reached. The temperature is then measured and recorded, and the operators of both cameras get into position. The operator of the gate gives a warning, empties the sand into the column of water, and releases the gate; the cameras then record the experiment. After at least one hour three cores are taken at two locations, one location at the viewing window (4.85 m from gate) and the second location 7.52 m from the gate, the purpose of these cores will be explained in a later section. The system is then set up for the next experiment.

Experimental Techniques

The movies were made using 16 mm Tri-X reversal film. Camera A was shot with an f-stop of 2.8, a filming speed of 64 frames/sec, and an auxiliary shutter opening of 1, producing an effective shutter speed of 1/500 sec. Camera B had an f-stop of 2, a filming speed of 64 frames/sec, and a shutter speed of 1/300 sec.

As described above two sets of sediment samples were taken following a run. Each set consists of three cores

aligned perpendicular to the flow direction and between 4-10 cm apart from each other. Polyethylene tubes with an ID of 2" and wall thickness of 1/8" were used to make the cores; for runs B and C the upstream direction was marked on the cores. The cores were labeled with the run number (the downstream set differentiated by adding a prime superscript) and lettered a, b, c with a on the left looking upstream. The a cores were then sectioned into slices approximately ten grain diameters thick and analyzed for sorting and grading trends by means of a settling tube. The remaining cores were impregnated with a waxless polyester resin to form a permanent record and to allow a structural and textural study to be made at a later date.

DESCRIPTION OF SEDIMENT TRANSPORT AND DEPOSITION

Though the most ideal way to assimilate information from the movies is to view the films first-hand, I will attempt to describe the most striking and important features in this section, as well as produce a basis from which the different runs can be compared and contrasted. For a more complete picture of the processes I will be describing, the films have been preserved in the M.I.T. archival collection.

One very minor part of the depositional sequence that occurred in every run, but which I will not describe, is the deposition of fine sediment from the last stagnant part of the flow. A brief summary of the initial conditions of each run is listed with the subheadings.

Run A-1 (D = 0.44 mm, H = 244 cm, C=20%)

As the flow impinged on the existing bed in this run, a number of peculiar things happened, most of which were probably related to air in the existing bed and the presence of the viewing window. The bed appeared to inflate and undergo internal deformation by jiggling of the bed, and then be eroded down about 0.75 cm. The first grains deposited on this erosional surface arrived "en masse" from a dense suspension and were transported for a short distance along the bed by shearing of the grains with little relative grain motion. At this point a good deal of air was noticeable in the flow.

The major part of the bed was deposited in thin planar bursts of sediment raining out of a dense suspension. The sheets were indistinguishable until only a short time before they were deposited, at which time they became only vaguely defined. As the flow evolved with time, the sheets became thinner and thinner until the grains were deposited in a tractional mode, characterized by grains rolling along the bed surface with extensive relative grain movements before coming to rest as part of the deposit. Approximately one-quarter of this deposit can be attributed to deposition by traction in a relatively sediment-free flow.

The thickness of this unit, measured from the lowest point of erosion, was 2.5 cm.

Run A-2 (D = 0.44 mm, H = 168 cm, C = 20%)

Erosion of about 0.5 cm of the existing bed again prefaced deposition; erosion was slow and continuous in this run. After the lowest level of erosion was reached, was a time lag before deposition began, during which a layer of grains about 1 cm thick was transported along the bottom by shearing before coming to rest; very little relative grain motion was noted.

The main part of the bed was deposited in thin planar bursts that rained out of suspension, though the bursts were less well defined in this run than in Run A-1. This part of the sequence can be further differentiated by an initial stage in which the bed was deposited very quickly, and a second stage, during which the bed was deposited half as rapidly. A continuous gradation from the planar bursting depositional mode to a tractional mode was again noted, with the last 0.5 cm of the bed deposited by grains in traction. At the test section this bed was 3.1 cm thick.

Run A-3 (D = 0.44 cm, H = 244 cm, C = 40%)

The top of the existing bed was not visible in this run so the style of erosion and the base of the initial deposit cannot be described. However, the part of the bed which was first seen to be deposited and which was presumably part of the first deposit arrived as a sheared mass approximately 1 cm thick. Again this sheared bed

was transported a short distance with little relative grain motions; active jiggling of the liquefied bed was also seen.

The second period of bed development was not totally unlike the equivalent period in the previous runs, but there were some noticeable differences. Perhaps a loose analogy for how this part of the bed was deposited is the pages of a book that are being fanned very rapidly and settling on the back cover; the bed accumulates in a rather diffuse manner with a certain degree of individuality preserved as the "sheet" or "page" settles. The bed also compacted and dewatered noticeably as this part of the bed was deposited.

Following this period, though, there was a hiatus during which little sediment was deposited. Then essentially the entire load left in suspension was deposited very quickly with development at the fluid-bed interface of a few small, asymmetric waves with steeply sloping downcurrent faces travelling downcurrent at a moderate speed. These waves were not too well developed, though their significance may be more fully realized in descriptions of later runs.

The final grains of the deposit were again grains rolling along the surface in traction; these grains were deposited as the current velocity waned. The entire bed was at least 3.3 cm thick.

Run A-4 (D = 0.44 mm, H = 168 cm, C = 40%)

The black sand at the viewing window that defines the existing bed was very effective in visualizing the development and extent of the erosional processes in this run. Shortly after the front of the surge passed over the existing bed the concentration of sediment at the base of the flow was large enough so that the basal layer behaved as a sheared bed. The shear was large enough that the bed continued to erode, resulting in the black sand becoming incorporated into the flow, but with very little vertical transport of material. Very shortly after the existing bed was eroded to its deepest level, about 1 cm of sediment was deposited in a very short time and with little subsequent grain movement, either absolute or relative.

The second period of deposition contributed to the bulk of the bed. Sediment was delivered to the bed in bursts so that the bed accumulation is more aptly described as thick planar bursts of suspension rather than thin planar bursts of sediment forming the deposit. As the surge evolved the bursts became less frequent until the bed-fluid interface was definable; this was followed by a period of very slow accumulation of sediment from suspension.

The bulk of the sediment still in suspension was delivered to the bed in a few ill-defined bursts that represent catastrophic release of suspension from the flow.

Grains were then transported at the bed surface by traction until the flow decreased enough to allow their deposition. This bed was about 3.0 cm thick.

Run B-1 (D = 0.54 mm, H = 168 cm, C = 40%)

Difficulties arose in trying to describe the erosional processes because the top of the existing bed lay beneath the viewing window, but the amount of erosion was presumably limited since the time interval between the arrival of the flow and deposition was not long.

The mechanism by which the first few grains of sand were deposited is not known since they were deposited below the field of view. However, most of the depositional event can be characterized as thick planar bursts of sediment raining out of the suspended load, followed by shearing of the bed such that the upper part of the layer was transported about 1 cm downcurrent while the base remains relatively stationary. These thick planar bursts arrived more or less continuously, though with a decreasing frequency as the flow progressed. A notable observation is that the flow carried numerous pockets of air mixed through the suspension, a result of air becoming entrained at the head of the surge.

After about three-quarters of the bed had been deposited, there was a discontinuity in the depositional sequence during which only a small fraction of the bed was

added. The remainder of the bed was deposited in a few bursts of sediment from suspension. A small amount of sediment was deposited during a period of tractional movement. The deposited bed was 3.8 cm.

Run B-3 (D = 0.54 mm, H = 244 cm, C = 20%)

Minor erosion of the existing bed was followed very quickly by deposition of the first grains from the flow. These grains formed a layer approximately 0.25 cm thick that were emplaced "en masse" with no absolute movement of the grains. There was then an interval of nondeposition during which grains directly above the depositional surface were transported as a shearing bed.

The majority, or about two-thirds of the bed, was deposited by a three-layer flow. Below the base of the bottom layer lay the deposited bed, defined as a region of no absolute grain motions, that changed continuously with time upward. The basal layer was a "zone of bed consolidation" which was essentially a sheared bed depositing grains onto the deposited bed. This layer delivered sediment to the zone of bed consolidation, and in so doing contributed to the top layer, or layer of relatively sediment-free flow. By the nature of this stratified flow it is understandable that sediment was delivered from the turbulent, sediment-rich layer to the zone of bed consolidation in bursts. Since this part of the flow

was so dynamic and the bed was deposited so quickly, thereby trapping extensive water in the bed, the deposited bed was jiggled extensively with grain motions predominantly in the horizontal plane.

The third period of deposition was gradational between the preceding period and the succeeding period. Grains were deposited continuously from suspension, then sheared along the bottom with little relative grain motion before coming to rest. This degraded into a more tractional mechanism that completed the depositional event.

The large globs visible in the movie are balls of sand that did not become disaggregated in the initial suspension. This bed was 3.9 cm thick.

Run B-4 (D = 0.54 mm, H = 168 cm, C = 20%)

The first layer of this deposit was laid down almost immediately following erosion of the existing bed. The lighting for this particular run was poor, but it appeared that this layer was deposited with little subsequent movement. A period of nondeposition occurred with grains deposited as a sheared bed along the bottom.

As in Run B-3 a three-layer flow developed with grains from the zone of bed consolidation contributing to about one-third of the bed thickness. This style of deposition evolved into one characterized by thin planar bursts of sediment raining out of suspension with little or no sub-

sequent movement once deposited on the bed.

The last major part of the bed was a result of the very rapid exhaustion of sediment in suspension; the suspension appeared to dissipate instantaneously. A relatively thick zone (∿0.25 cm) of grains transported by traction developed during the last period of the flow. This run deposited a bed 2.5 cm thick.

Run B-5 (D = 0.54 mm, H = 244 cm, C = 40%)

The existing bed was only slightly eroded; erosion was followed very quickly by deposition of a bed about 0.5 cm thick. The first bed was emplaced as a mass from suspension and was not transported after deposition.

The second period of deposition was again characterized by a three-layer flow with grains deposited from a zone of bed consolidation. Turbulent eddies from the sediment-rich turbulent layer impinged on the lower layer, sometimes almost to the bed surface. This mechanism may be partly responsible for jiggling of the liquefied bed; at some points the bed shook violently, though with no noticeable transportation of grains. The depositional style gradually evolved into one characterized by thin planar bursts of sediment raining out of suspension. The last period of deposition involved a thick layer of grains

transported and deposited in a tractional mode. The thickness of this bed was 4.5 cm.

Run C-1 (D = 0.25 mm, H = 244 cm, C = 20%)

This run provided a bounding limit for the experiments; the net effect of the surge was erosive. The existing bed eroded relatively slowly before it passed from the field of view at the viewing window; the level of the bed deposited never reached above this point. The flow was most convincingly turbulent, with a good deal of air entrained in the flow. The movies show an upward transport of material at the viewing section, presumably the effect of the viewing window. A large part of the end of the surge was sediment-free while maintaining an appreciable flow thickness ($\sim$8 cm).

Run C-2 (D = 0.25 mm, H = 168 cm, C = 20%)

This run was also extensively erosive, but the net change in the bed height was positive. The first part of the surge eroded the existing bed below the bottom of the viewing window so the first-deposited grains were not observed.

During the major part of the flow no sediment was deposited, and particles appeared to be suspended evenly throughout the flow. In a very short period of time the

suspension was catastrophically released from the sediment-laden flow to form a liquefied bed and a relatively clear flow. Development of waves at the fluid-bed interface was associated in time with mass deposition occurring when the interface became identifiable. At a particular point the bed expanded as the crest of a wave passed and contracted as the trough passed; the bed appeared to be inhaling and exhaling. These asymmetric waves travelled downstream at a moderate rate. The wave amplitude decreased and the frequency increased with time until the waves disappeared altogether and the deformable sediment settled to a horizontal planar surface.

In the time between the beginning of the release of the sediment from suspension and development of waves, an interesting property was noticeable in the upper part of the suspension. Assuming a vertical z-axis with a fixed origin to be superposed at a point in the flow, the sheared sediment was observed to exhibit an increase in $\partial U/\partial z$ of the grains within the sediment layer with time. U of the grains decreased as the flow evolved, but not as quickly as the thickness of the layer of transported grains.

The last period of the depositional process was characterized by grains being transported and deposited by traction. The thickness of this bed at the viewing window was at least 1.8 cm.

Run C-3 (D = 0.25 mm, H = 244 cm, C = 50%)

The existing bed was eroded about 0.5 cm before a basal layer 0.25 cm thick was deposited very quickly as a massive layer. A bed approximately 1.5 cm thick developed on top of the basal layer with grains transported downcurrent by shearing of the bed, the shear resulting from a turbulent, concentrated flow passing above. The interface between the turbulent and the sheared layers was rather well defined and had no net change in the z-direction with time, except for local fluctuations due to turbulent eddies impinging on the interface; turbulent eddies ranged up to 2 cm across.

Suddenly the sediment in suspension in the turbulent layer of the flow rained onto the bed, freezing the sheared layer and causing part of the turbulent layer to become a sheared bed. Another two-layer flow developed, with the turbulent layer being essentially sediment-free. When the interface between the two layers became discernible, asymmetric waves developed. These waves were similar to the ones described in Run C-2, though more numerous. A range of wave forms was also seen, from slightly asymmetrical waves to breaking waves. These waves decreased in amplitude and increased in frequency with time. The decay of the waves also represented the decay of the sheared bed, which rigidified continuously from bottom to top. The speed of these waves ranged from about 40-60 cm/sec, as

calculated from the movies. Interference of the waves was a result of different waves travelling at different speeds and interacting with each other. A rough estimate of the wavelength is 8 cm. These interfacial instabilities were also observed to be of a higher frequency than waves at the free surface.

The final grains were deposited as grains rolled along the bed came to rest, contributing only a small part to the total thickness of 5 cm.

Run C-4 (D = 0.25 mm, H = 168 cm, C = 40%)

Erosion of the existing bed did not proceed evenly and continuously as in most of the other runs; instead, a scour trough developed that slowly proceeded downcurrent. This erosional feature made it difficult to identify the style of deposition of the first grains, though it appeared that a thin blanket froze out of suspension onto the erosional surface.

A two-layer flow similar to the one described in Run C-3 developed, characterized by a lower, thick, sheared layer and an upper, turbulent, sediment-rich layer. As sediment rained from suspension to form a sheared bed and a sediment-free turbulent flow, interfacial waves again developed in the same manner as the previous two runs. As the waves decreased in amplitude, the sheared bed de-

creased in thickness as it froze from the bottom upward.

The final period of deposition involved grains in traction, again contributing marginally to the bed thickness of 3.1 cm.

DISCUSSION

Three distinct styles of deposition were identified in an earlier section: (1) deposition of grains transported by traction, (2) deposition of grains by settling from the fluid suspension, and (3) deposition by mass emplacement (J. Southard, personal communication). It was also noted that a continuum exists between these end-members.

One approach to examining the depositional styles represented in each experiment is to locate these styles in the continuum, compare the conditions of experiments exhibiting similar styles, and to relate grain size, concentration, and velocity to depositional style.

Depositional Styles

A minor part of each deposit was a result of grains deposited from traction as the current waned. Absolute thickness of layers due to traction are greatest in the B-series, with Runs B-3 and B-5 being exceptional. Runs A-1 and A-2 also deposited a significant thickness of grains by traction. In terms of relative thickness of layers (i.e. comparing thicknesses as a function of number of grain diameters), it appears that the B-series stands out because this series appears to produce the thickest layers,though this conclusion is subjective. Thickness is

also difficult to estimate because in most runs no clear distinction could be made between the tractional mechanism and the preceding mechanism; the change in style was often gradational.

Three distinct styles of deposition recognized in the experiments can be characterized as settling from suspension. At this point it is necessary to define the bed as a region of no absolute grain motion; a liquefied bed jiggled by outside forces may still be considered a bed as long as no net translation of grains occurs. The style of deposition will be defined as the means by which the grains ultimately come to rest.

Runs A-3, A-4, B-1, and B-4 exhibited deposition of sediment from suspension. At a point in the flow an undescribed event triggered a mechanism that released essentially all of the sediment remaining in the flow. The sediment rained onto the bed to form the deposit in a very short time.

A somewhat different style of deposition from suspension is the delivery of sediment to the bed from the turbulent flow by thin planar bursts of sediment (Runs A-1, A-2, B-4, and B-5). The bed is added to in a discontinuous fashion, though the bursts are ordered in time. This style tends toward a bed deposited by mass emplacement because the presence of a layer of sediment of finite thick-

ness limits the mobility of an individual grain.

Runs A-3 and A-4 deposited layers as thick planar bursts from suspension, the next step in the continuum between deposition from suspension and deposition by mass emplacement. The deposit in Run B-1 was formed as a combination of the two end-members; sediment was delivered to the bed as a thick planar burst, but while the base of the layer remained stationary, the top part was transported downcurrent by shearing of the bed for a short distance before the bed froze (deposited by mass emplacement).

The three-layer flow developed in Runs B-3, B-4, and B-5 deposited the sediment in a mass emplacement mode. The base of the sheared layer moved upward continuously in time as sediment was added to the top of the layer from the turbulent, sediment-rich layer above. Grains in the sheared bed experienced fewer and fewer absolute motions as time progressed until they were frozen in the bed. Since grains that entered the sheared layer tended to remain there, the layer can be thought of as a kind of bed. Delivery of material to this "bed" was by deposition from suspension. So in one respect the bed can be thought of as forming as a result of two, different, distinctive styles of deposition occurring simultaneously.

The two-layer flow in Runs C-3 and C-4 also deposited a bed by mass emplacement. The difference between this two-layer flow and the three-layer flow described above

is that the sheared layer does not change significantly in time. The sheared layer freezes as a whole unit at a point when the flow decreases.

Another example of depositional style characterized by mass emplacement is Run C-2; the bed forms as a sheared bed freezes. The sheared bed develops as sediment raining out of suspension traps enough water to form a liquefied bed; this bed is then sheared as the current continues to flow. So in one respect a bed formed by deposition from suspension is modified by the flow to form a deposit by mass emplacement. It seems possible, though, that some of the characteristics of deposition from suspension may be perserved in the final deposit. The final two-layer flow developed in Runs C-3 and C-4 is essentially analogous in depositional style.

The first grains deposited in the A and B series were also deposited by mass emplacement. Near the front of the surge a layer up to 1 cm thick developed that was sheared along the bottom. At some point the shearing ceased, the bed froze, and another style of deposition developed. In the C series, on the other hand, the first grains were deposited by mass emplacement, but in a more idealized manner; a mass of grains appeared to arrive in an instant and form the bed.

Corelation of Depositional Styles

Deposition from a tractional mode is present in all runs, but deposition is not equivalent in all cases. It seems that grain size and concentration play the most significant roles. A large grain size and a low concentration allow a substantial part of the sediment load to be deposited while the competence of the current remains high. A higher velocity seems to contribute to this end in a more subtle manner.

An examination of the depositional styles for the bulk of the deposits yields a grouping of styles with grain size the major controlling factor. The fine-grained sands appear to have been deposited predominantly by mass emplacement, while the medium-grained sands were deposited almost exclusively by settling from suspension. The coarser sands were strictly deposited by a mass-emplacement mechanism, but initially by settling from the suspended load.

It is not difficult to see how fine sands would be deposited by mass emplacement and coarser sands not, since the finer sands are more easily kept in suspension. It must be noted that while the coarser sand was deposited by mass emplacement, the style was not the same. In the finer sands a layer of appreciable thickness froze over a

very short time, while in the coarser sands the bed was augmented in small accretionary steps, or by accretionary mass emplacement. Why no mass emplacement mechanism was observed in the medium sands is not clear. The distinction between styles of deposition in coarse and medium sands is confusing.

When one tries to distinguish styles of deposition as a function of velocity or concentration, no clear pattern emerges. These variables certainly alter the deposit in detail, but even as second-order effects, velocity and concentration appear to play no major role on a larger scale.

Within a particular grain size, concentration appears to play a greater role than velocity. In the medium sands the low-concentration runs deposited sediment from bursts of suspension only, while in the high-concentration runs sediment was deposited as a result of the rapid dissipation of the suspended load in addition to deposition from bursts of suspension. The fine sands also showed a marked distinction between high and low concentration. The high-concentration runs were characterized by a much more complex depositonal style.

Coarse sands do not show an obvious difference in depositional style between high-concentration and low-concentration surges. The effect of the grain size as discussed earlier appears to control the style of deposition.

Erosional Characteristics

Two characteristics are manifested as a surge erodes the existing bed. For a given velocity and concentration, the fine snads are eroded much more deeply than the coarse sands. This result is perhaps obvious, but worth mentioning. The other point is that low-concentration surges erode more material than high-concentration surges. This too, is obvious in light of a flow-capacity argument.

The reason for stating these points is to prove the existence of a fully turbulent surge. An examination of the flow depth profiles in Figures 6 and 7 reinforces this argument.

Bed Thickness

It is difficult to discuss bed thickness to any great extent because the measure of bed thickness is one dimensional. An obvious argument for the changes noted includes the flow competence. The coarse sands are transported and spread evenly over a much smaller area than the fine sands. Concentration obviously affects the competence of the flow, as well as the velocity, but the relative significance of each factor cannot be evaluated from the data.

Inertial Instabilities

The waves produced at the fluid-bed interface in Runs A-3, C-2, C-3, and C-4 were a result of two streaming two-phase fluids of different densities flowing at different

FIGURE 6: Flow Depth Profiles for
Runs A-3, B-1, B-3, B-4, B-5.

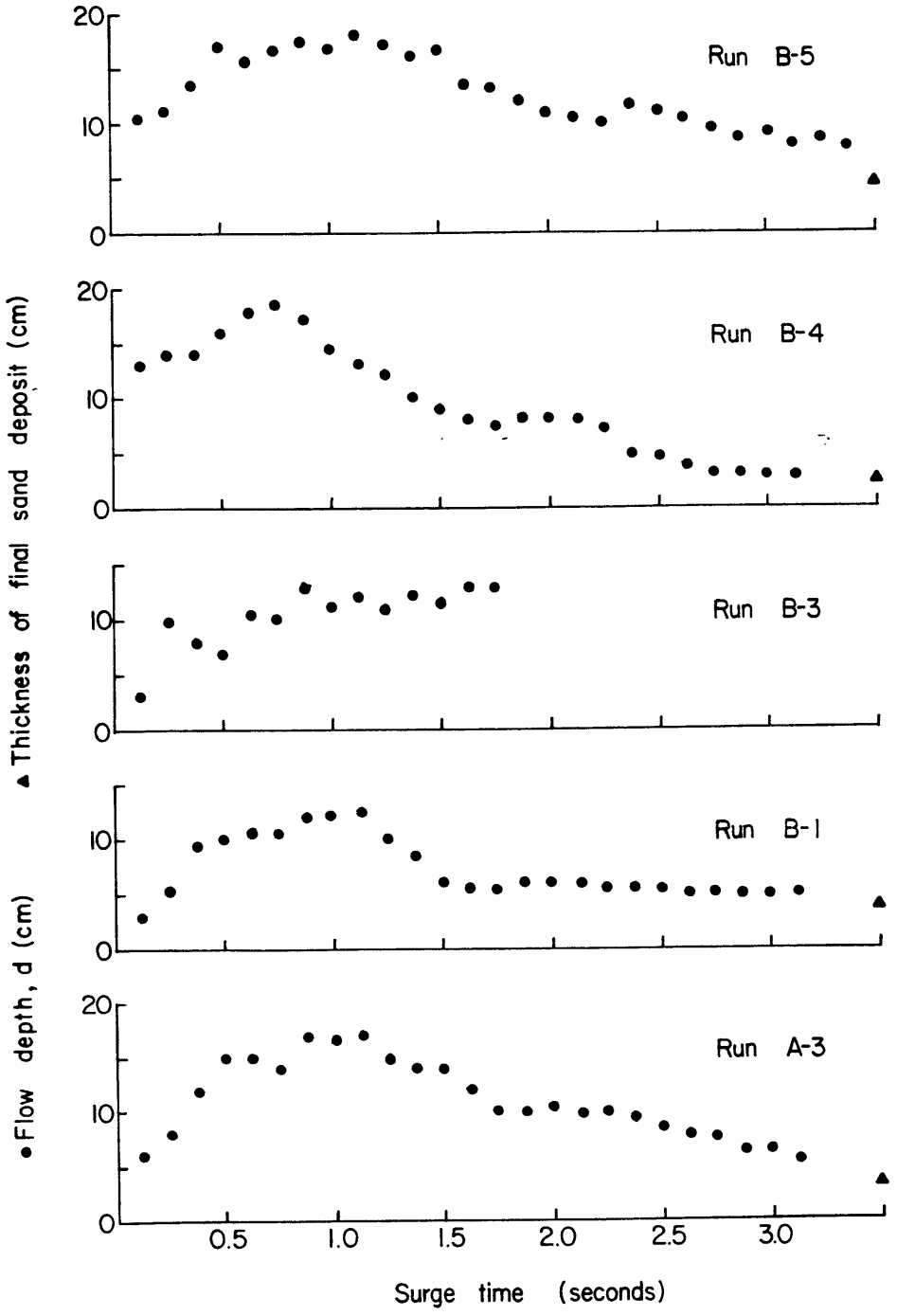
Run B-5
Run B-4
Run B-3
Run B-1
Run A-3
20
10
0
0.5
1.0
1.5
2.0
2.5
3.0
▲ Thickness of final sand deposit (cm)
• Flow depth, d (cm)
Surge time (seconds)

Figure 6

FIGURE 7: Flow Depth Profiles for Runs C-1, C-2, C-3, C-4.

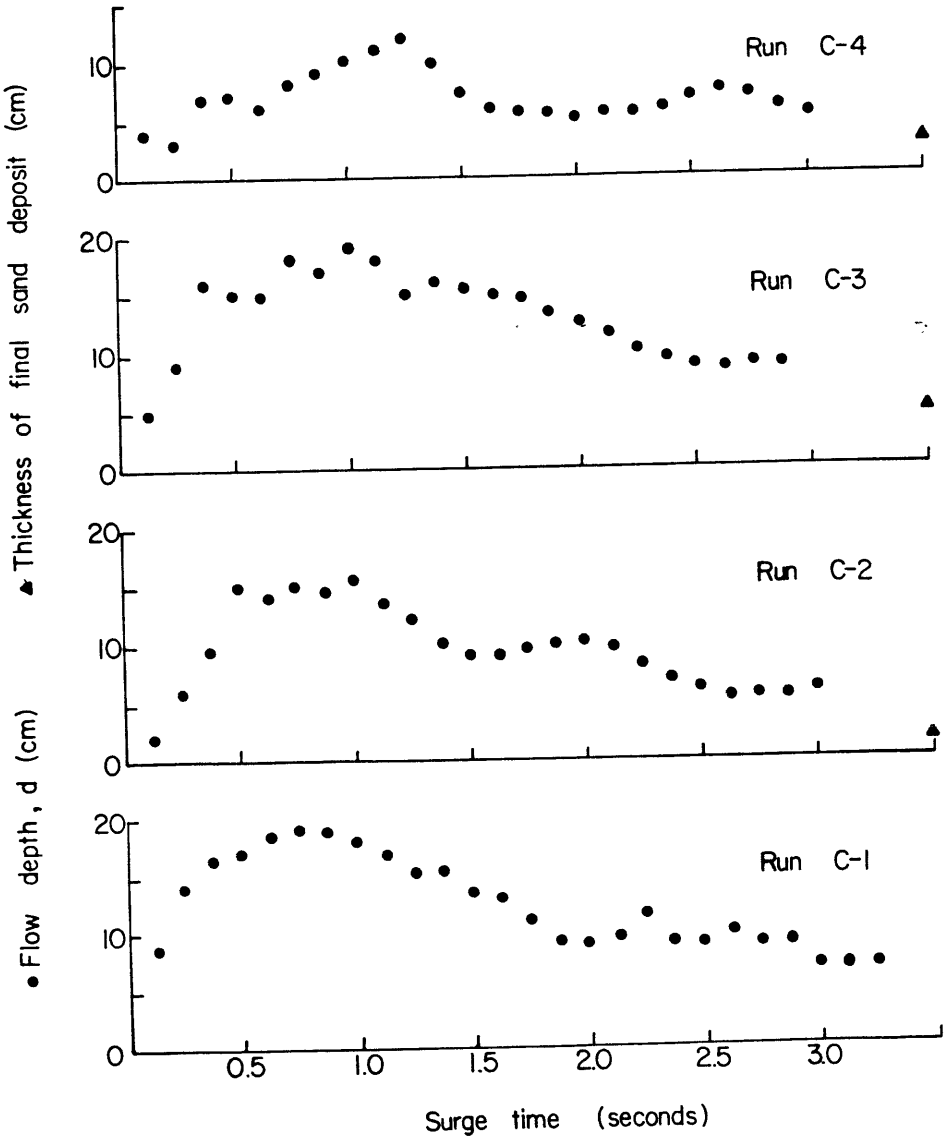
Run C-4
Run C-3
Run C-2
Run C-1
10
0
20
10
0
20
10
0
20
10
0
0.5
1.0
1.5
2.0
2.5
3.0
Surge time (seconds)
▲ Thickness of final sand deposit (cm)
● Flow depth, d (cm)

Figure 7

velocities past each other; the implicit assumption in this argument is that a sheared liquefied bed can be treated as a viscous fluid. The instabilities developed in systems in which the velocities and the densities of both "fluids" changed with time.

In order to discuss the parameters controlling the formation of these instabilities, an effort must be made to analyze their development qualitatively. Given the conditions under which these instabilities develop, one immediately thinks of Kelvin/Helmholtz waves as dicussed by Birkoff (1962). Yih (1969) has given an analysis of Helmoholtz waves developed in a steady flow and has produced a criterion for their formation. The criterion is

$$\rho_1\rho_2\left(\frac{U_1-U_2}{\rho_2+\rho_1}\right)^2 > c_o^2$$

where

$$c_o^2 = \frac{g}{k}\frac{\rho_2-\rho_1}{\rho_2+\rho_1} + \frac{Tk}{\rho_2+\rho_1} .$$

ρ_1 and ρ_2 are the density of the two fluids, U_1 and U_2 are the velocities of the two fluids, c_o is the speed of the waves in the absence of the currents represented by U_1 and U_2, k ($k = \frac{2\pi}{\lambda}$) is the wave number, and T is some value of the surface tension.

The waning stages of the surge are by no means steady, but it may be reasonable to view changes in the density and velocity as negligible when compared to the time nec-

essary to develop the vortices of the instabilities (C. Wunsch, personal communication). Therefore, after dismissing the effects of surface tension at the interface, values of ρ_1, ρ_2, U_1, U_2 and λ can be substituted into the criterion to test if the presence of Helmholtz waves is possible. For values of ρ_1 = 1.05 g/cm^3, ρ_2= 2.25 g/cm^3, U_1 = 100 cm/sec, U_2= 20 cm/sec, and λ= 8 cm; c_o^2 is 454 (cm/sec)^2, c_o is 21 cm/sec, and $\rho_1 \rho_2 \left(\frac{U_1-U_2}{\rho_2+\rho_1}\right)^2$ is 1388 (cm/sec)^2. The velocity function is certainly larger than c_o^2, though less than an order of magnitude. The value of c_o also seems reasonable, so it seems qualitatively possible to assume that Helmholtz waves can be developed under the given conditions.

By studying the stability criterion, it is apparent that the velocity difference has a destabilizing effect on an interface while the density contrast tends to stabilize the interface. For example, if the density values for the experiments are kept constant, Helmholtz waves will persist until a velocity difference of 45 cm/sec is obtained.

An interface instability between a liquefied bed and a current can be produced experimentally, and it seems probable that natural systems could produce similar features. The most important ramification of such an occurrence is in the area of syndepositonal deformation of the deposited bed. It is easy to imagine how a graded deposit could be re-

arranged by a wave passing at the top of the bed, especially in the case of a breaking wave.

Since waves did not develop in every run, it might be useful to relate the cases in which waves did occur to determine controls on the generation of waves. First, waves were generated in essentially every run with the finest sand; Run C-1 did not deposit enough sediment for these mechanisms to develop. The only other run in which instabilities developed was Run A-3, with the medium-sized sand.

It seems obvious then that grain size is the controlling factor in wave generation. Grain size must control the density difference strongly enough that a coarser sand will settle out of suspension too quickly to allow waves to develop. The larger grain sizes will also have well developed passages connecting pore spaces, making it difficult to trap water in the bed and reduce the density difference; remember that an increased density difference stabilizes the interface.

It also appears that the concentration plays a role in the development of instabilities. This is probably best explained by the ability of a high-concentration of sediment settling out of suspension as a mass to trap water between grains more efficiently than a low concentration. This

will again reduce the density difference and destabilize the interface.

Velocity must also play some role, since waves are much better developed in Run C-3, a high-velocity run, than in Run C-4, a low-velocity run. The distinction is not too straightforward, since a higher concentration of sediment was used in Run C-3.

The question of interfacial instabilities as applied to sedimentology and soft-sediment deformation certainly requires more research before its potential significance and an understanding of the mechanisms involved can be fully realized. This report has primarily identified areas of physical conditions that could be potentially valuable to study.

CONCLUSIONS

Five major points can be made as a result of the experiments. Most of these points define styles of deposition in a high-velocity surge, a type of flow not well studied with respect to deposition of sands. These results also suggest that a re-examination of the mechanisms involved in different types of high-velocity surges must be made.

If deposition of sand from a high-velocity surge can be described by one of three depositional modes--by traction, by settling from suspension, or by mass emplacement--then the experiments reveal that the bulk of a deposit is a result of mass emplacement settling from suspension, and only a minor part of each deposit results from grains in traction.

The second point is that grain size plays the largest role in determining styles of deposition. Fine sands are deposited primarily by mass emplacement, coarse sands are deposited by accretionary mass emplacement with sediment delivered to the sheared layer by deposition from suspension, and medium sands are deposited mostly by sediment raining out of suspension.

Concentration plays a significant role if the grain size does not change. Surges of 40% and 20% volume concentration of sediment exhibit different depositional style for fine and medium sand. Coarse sand does not

appear to show any obvious variation in depositional style with these sediment concentrations.

Many ideas that have been generated to explain observed features in deposits from high-velocity surges may need to be re-examined. The notion of a "traction carpet" (Dzulynski and Sanders, 1962) may need to be revised or abandoned altogether. For instance, the processes that Walker (1967) described to generate proximal and distal turbidite deposits do not appear to be present in the laboratory study.

The final point is that several mechanisms were observed to occur in high-velocity surges that could easily reorganize a deposited bed. Interfacial instabilities, perhaps Helmholtz waves, were observed to actively alter bed thickness locally over a very short time span. Turbulent eddies impinging on a liquefied bed occasionally cause the bed to jiggle like a bowl of jelly. These processes need to be further investigated to determine if deformational processes could be attributed to them.

REFERENCES

Bagnold, R.A. 1956, The flow of cohesionless grains in fluids, Phil. Trans., Roy. Soc. London, 249, Ser. A, p. 234-297.

Birkhoff, G. 1962, Helmholtz and Taylor instability, Proc. Symp. Appl. Math., 13 (Hydrodynamic instability) p. 55-76.

Bouma, A.H. 1962, Sedimentology of Some Flysch Deposits, Elsevier Publ. Co., Amsterdam, 168 p.

Buckingham, E. 1914, On physically similar systems; illustrations of the use of dimensional equations, Phys. Rev., 4, p. 345-376.

Dzulynski, S. and Sanders, J.E. 1962, Current marks on firm mud bottoms, Conneticut Acad. Arts Sci., Trans., 42, p. 57-96.

Fox, R.W. and McDonald, A.T. 1978, Introduction to Fluid Mechanics, John Wiley and Sons, N.Y., 684 p.

Kuenen, Ph.H. 1950, Turbidity currents of high density, 18th Intl. Geol. Congress, London, Repts. Part 8, p. 44-52.

Kuenen, Ph.H. 1951, Properties of turbidity currents of high density, Soc. Econ. Paleontologists and Mineralogists, Spec. Publ. 2, p. 14-33.

Kuenen, Ph.H. 1953, Significant features of graded bedding, Bull. Am. Assoc. Petrol. Geologists, 37, p. 1044-1066.

Kuenen, Ph.H. and Migliorini, C.I. 1950, Turbidity currents as a cause of graded bedding, J. Geol., 58, 91-127.

Komar, P.D. 1977, Computer simulation of turbidity current flow and the study of deep-sea channel and fan sedimentation, in, The Sea: Ideas and Observations on Progress in the Study of the Seas, E.D. Goldberg, ed., p. 603-621, John Wiley and Sons, N.Y.

Leatherman, S.P. 1977, Overwash hydraulics and sediment transport, Coastal Sediments, '77, ASCE/Charleston, S.C., p. 135-148.

Menard, H.W. 1964, Marine Geology of the Pacific, McGraw-Hill Book Co., N.Y., 271 p.

Middleton, G.V. 1967, Experimental study of density and turbidity currents, III, Deposition of sediment, Can. Jour. Earth Sci., 4, p. 475-505.

Middleton, G.V. 1970, Experimental studies related to problems of flysch sedimentation, in Lajoie, J. (ed.), Flysch Sedimentology in North America, Geol. Assoc. Canada, Spec. Paper 7, p. 253-272.

Prandtl, L. 1952, Essentials of Fluid Dynamics, Hafner Publ. Co., N.Y., 452 p.

Southard, J.B. 1966, Turbulence and momentum transport in flow between concentric rotating cylinders, PhD thesis, Harvard Univ., Cambridge, MA, 126 p.

Southard, J.B., Boguchwal, L.A., and Romea, R.D. 1980, Test of scale modelling of sediment transport in steady unidirectional flow, Earth Surf. Proc., 5, p. 17-23.

Walker, R.G. 1967, Turbidite sedimentary structures and their relationship to proximal and distal depositional environments, J. of Sed. Pet., 37, p. 25-43.

Walker, R.G. 1970, Review of the geometry and facies organization of turbidites and turbidite-bearing basins, in Lajoie, J. (ed.), Flysch Sedimentology in North America, Geol. Assoc. Canada, Spec. Paper 7, p. 219-251.

Yih, C.S. 1969, Fluid Mechanics, McGraw-Hill Book Co., N.Y., 622 p.

LIST OF PLATES

PLATE I

a.

b.

PLATE II

a.

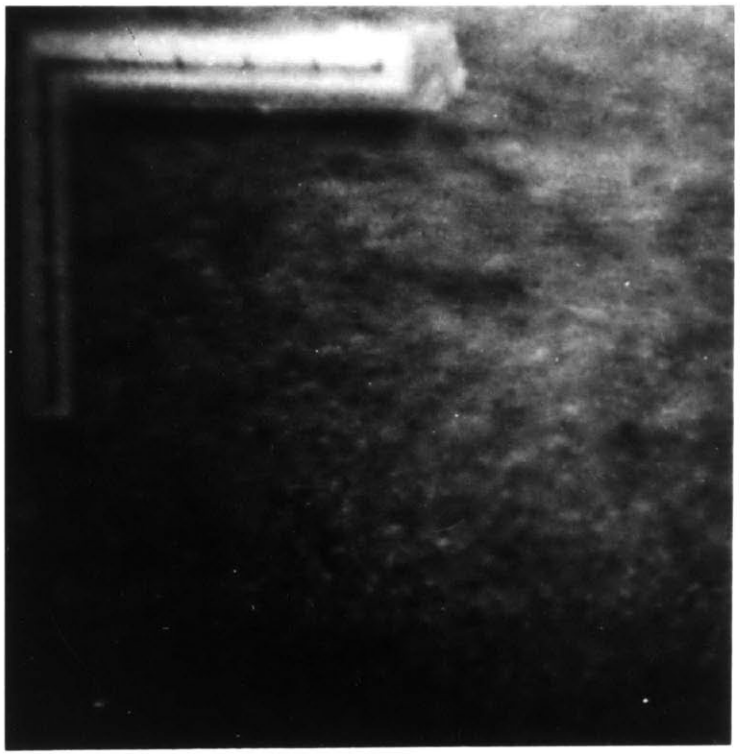

b.

PLATE III

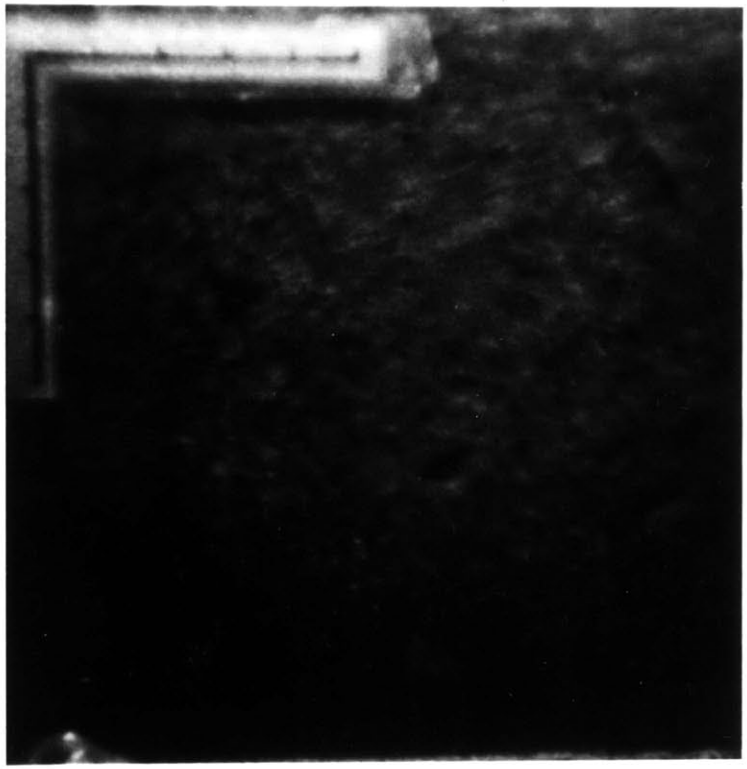

a.

b.

PLATE IV

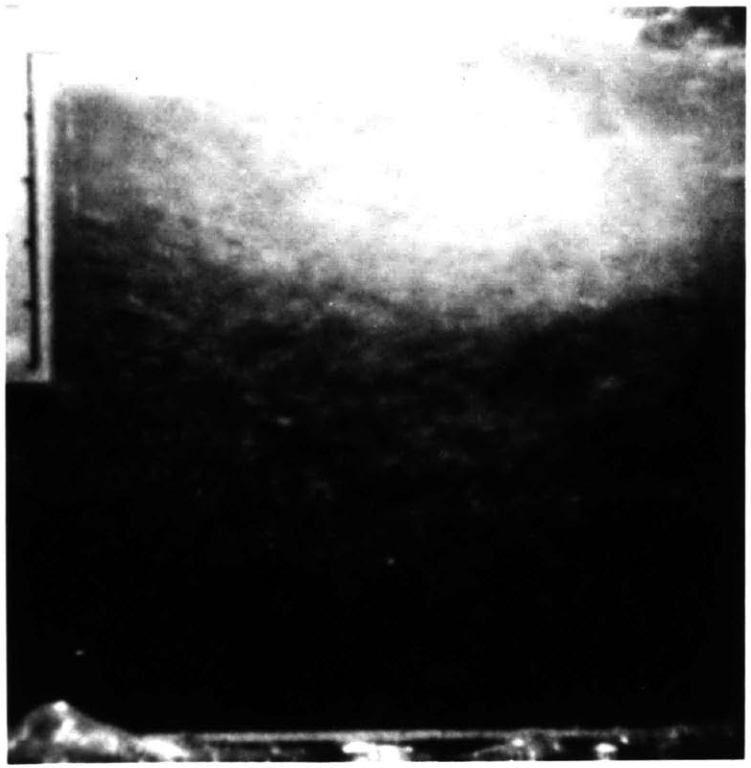

a.

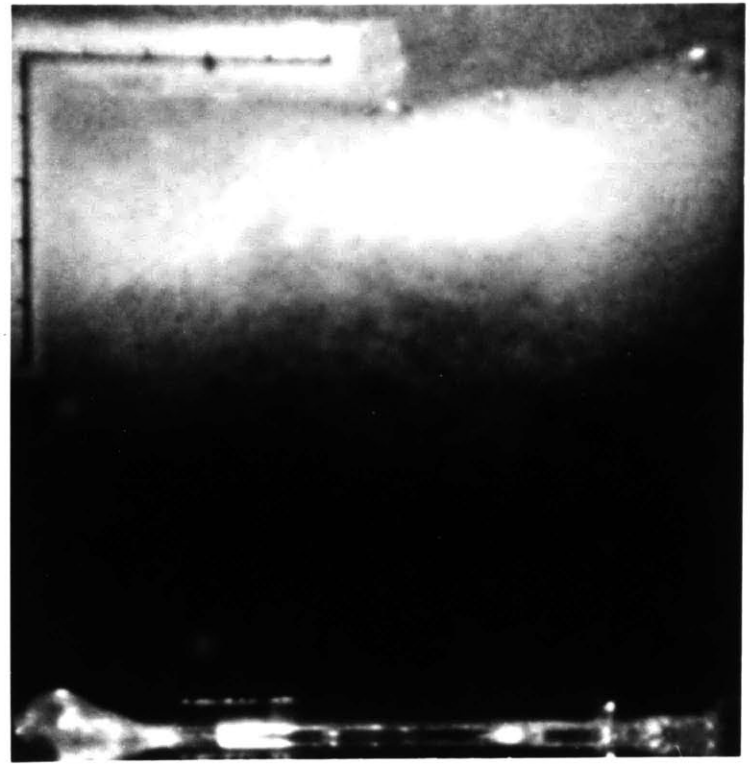

b.

PLATE V

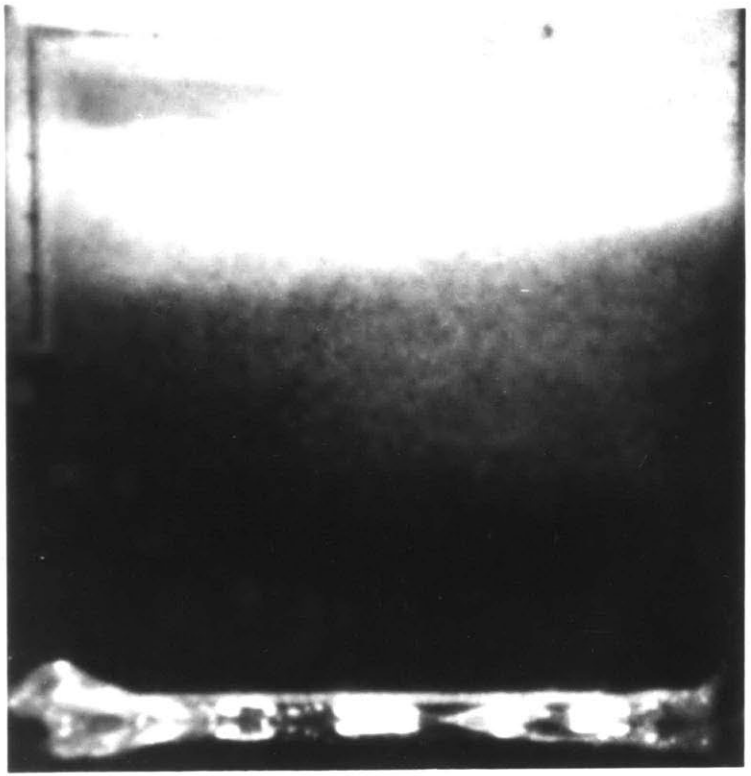

a.

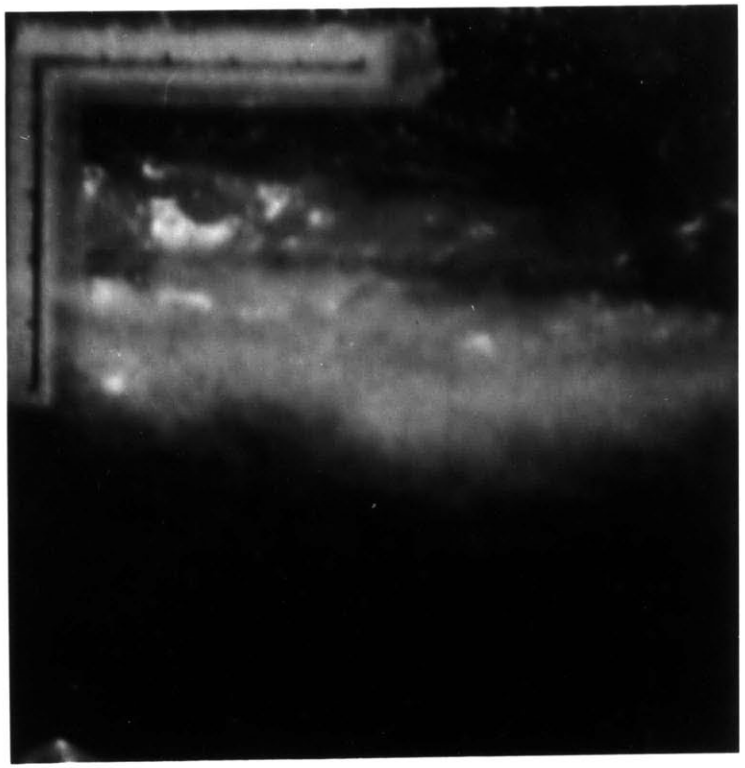

b.

PLATE VI

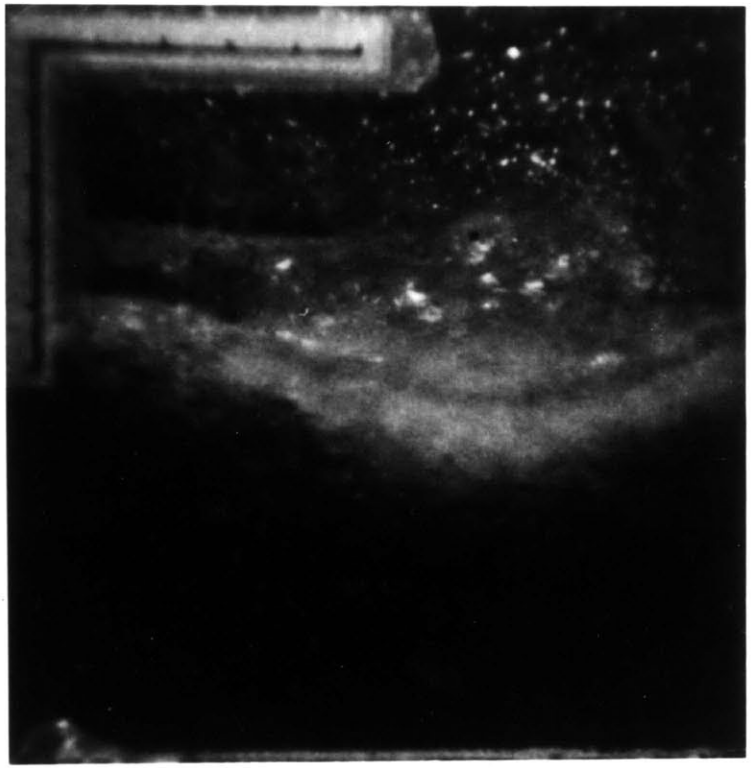

a.

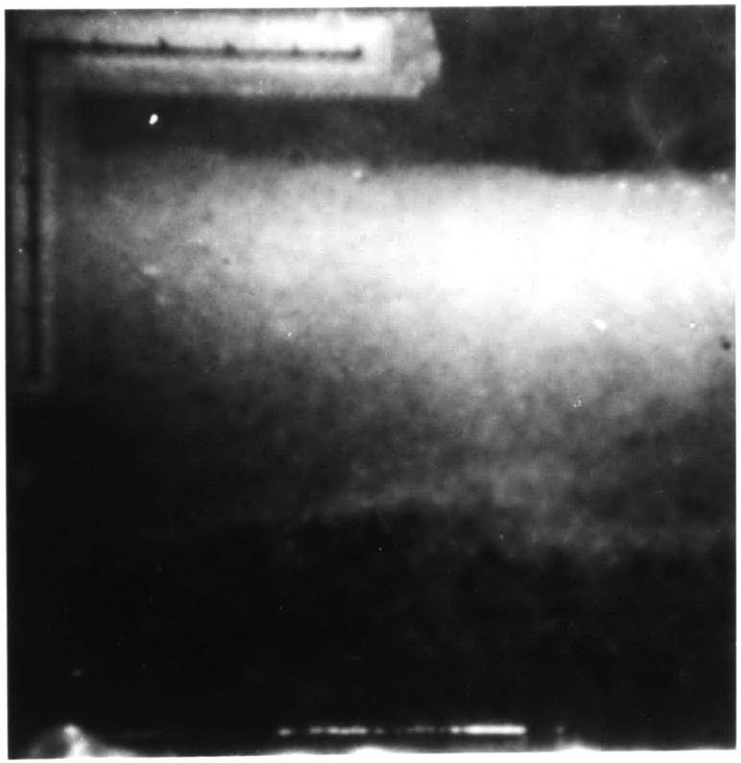

b.

PLATE VII

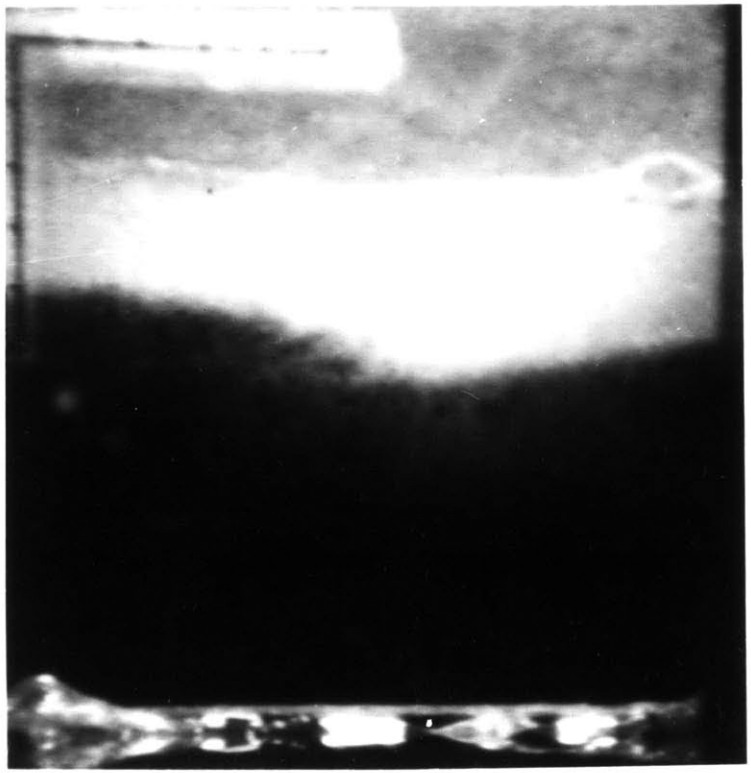

a.

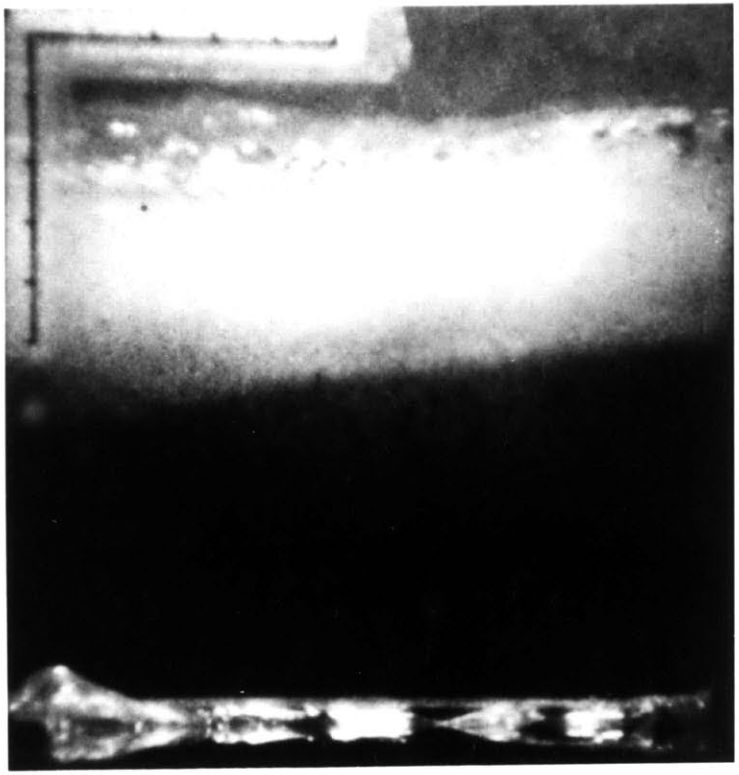

b.

PLATE VIII

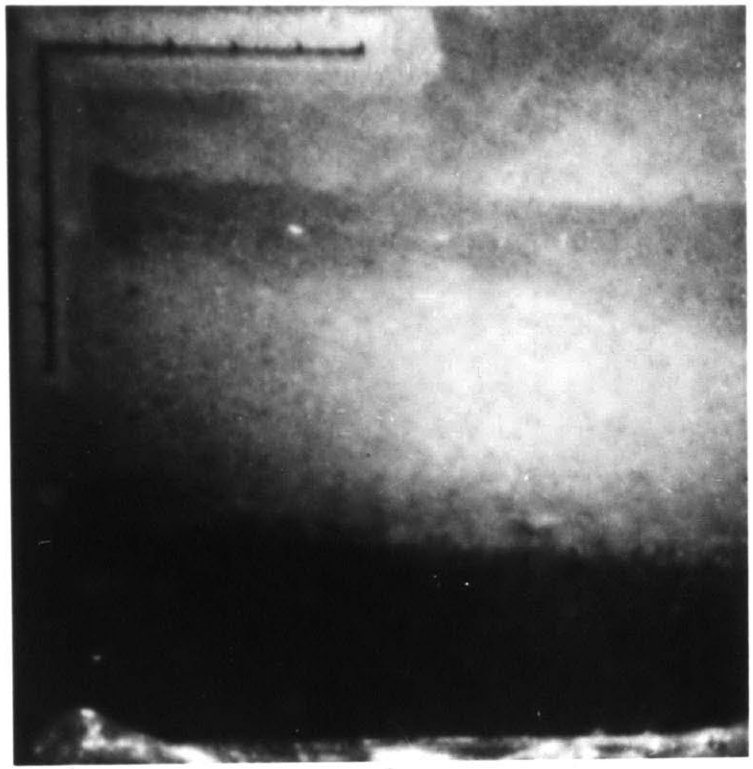

a.

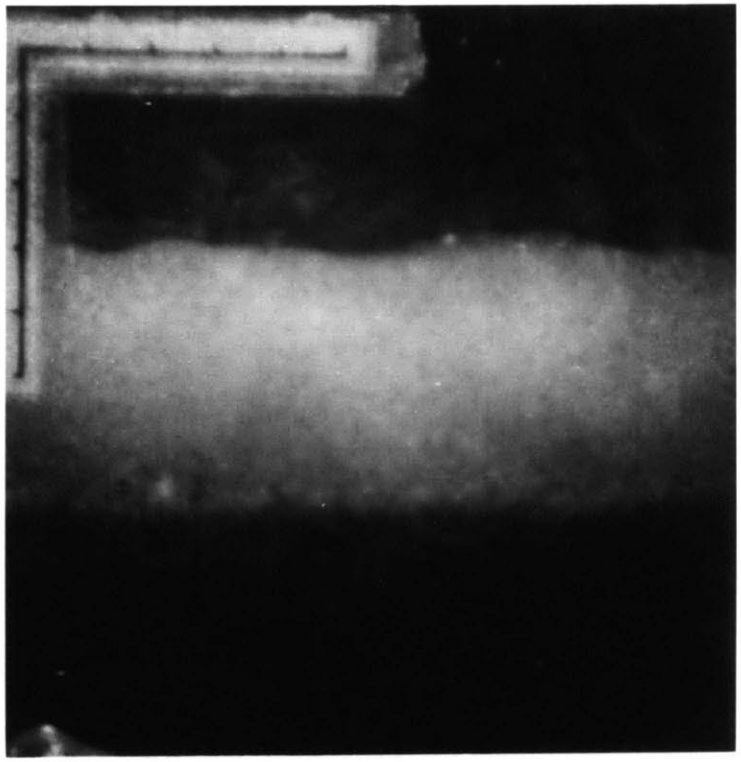

b.

PLATE IX

Run / Frame	A-3	B-1	B-3	B-4	B-5	C-1	C-2	C-3	C-4
0	0	0	0	0	0	0	0	0	0
8	6	3	3	13	10.5	8.5	2	5	4
16	8	5.5	10	14	11	14	6	9	3
24	12	9.5	8	14	13.5	16.5	9.6	16	7
32	15	10	7	16	17	17	15	15	7
50	15	10.5	10.5	18	15.5	18.5	14	15	6
48	14	10.5	10	18.5	16.5	19	15	18	8
56	17	12	13	17	17.5	19	14.5	17	9
64	16.5	12	11	14.5	16.5	18	15.5	19	10
72	17	12.5	12.	13	18	17	13.5	18	11
80	15	10	11	12	17	15	12	15	12
88	14	8.5	12	10	16	15.5	10	16	10
96	14	6	11.5	9	16.5	13.5	9	15.5	7
104	12	5.5	13	8	13.5	13	9	15	6
112	12	5.5	13	7.5	13	11	9.5	14.5	5.5
120	10	6		8	12	9	10	13.5	5.5
128	10.5	6		8	10.5	9	10	12.5	5
136	10	6		8	10.5	9	9.5	11.5	5.5
144	10	6		8	10.5	9	9.5	11.5	5.5
152	10	5.5		7	10	11.5	8	10	5.5
152	9.5	5.5		5	11.5	9	7	9.5	6
160	8.5	5.5		4.5	11	9	6	9	7
168	8	5		4	10.5	10	5.5	8.5	7.5
176	7.5	5		3	9.5	9	5.5	9	7
184	6.5	5		3	8.5	9	5.5	9	6
192	6.5	5		3	9	7	6		5.5
200	5.5	5		3	8	7			
209					8.5	7			
216					8				